

University of Natural Resources  
and Life Sciences, Vienna

Department of Sustainable  
Agricultural Systems  
Division of Livestock Sciences



# **Molecular Characterization of ZC3H11A Functions and Expression Patterns During Embryonic Development**

Shady Younis

Supervisor

Prof. Göran Andersson, Swedish University of Agricultural Sciences (SLU).  
Prof. Leif Andersson, Uppsala University.  
Dr. Elizabeth Ruth Gilbert, Uppsala University.  
Dr. Göran Hjälm, Uppsala University.

Co – Supervisor

Prof. Johann Sölkner, University of Natural Resources and Life Sciences, Vienna.

Vienna, June 2011

<b>Abstract</b> .....	<b>3</b>
<b>Introduction (Literature review)</b> .....	<b>4</b>
<b>Muscle development</b> .....	<b>5</b>
Myogenesis.....	5
Fiber types .....	5
Myogenic Regulatory Factors .....	6
IGFs in muscle development.....	8
<b>ZBED6 transcription factor</b> .....	<b>9</b>
<b>ZC3H11A, zinc finger protein</b> .....	<b>10</b>
<b>Splicing machinery</b> .....	<b>12</b>
<b>Aim of thesis</b> .....	<b>15</b>
<b>Materials and methods</b> .....	<b>18</b>
<b>Results</b>	
<b>RNA quality and purity</b> .....	<b>22</b>
<b>The effects of silencing ZC3H11A in C2C12 cells</b> .....	<b>23</b>
<b>Does silencing of ZC3H1A affect the differentiation of myoblasts?</b> .....	<b>26</b>
<b>Is ZC3H11A involved in RNA splicing?</b> .....	<b>27</b>
<b>ZC3H11A cellular localization</b> .....	<b>29</b>
<b>ZC3H11A protein expression pattern during embryo development</b> .....	<b>30</b>
<b>Discussion</b> .....	<b>31</b>
<b>Conclusion</b> .....	<b>34</b>
<b>References</b> .....	<b>36</b>

**Abstract:**

The previous discovery of a single nucleotide substitution in intron 3 of the insulin-like growth factor 2 (*IGF2*) gene in pigs revealed a novel mechanism for regulation of muscle growth. This mutation disrupts binding of a transcription factor, *ZBED6*. This domesticated DNA transposon is located within the first intron of *ZC3H11A* gene, which encodes a poorly characterized zinc finger binding protein. In this project, we attempted to characterize the expression patterns and biological function of *ZC3H11A*. We hypothesized that *ZC3H11A* may play a role in RNA splicing and muscle development. *ZC3H11A* was silenced in mouse myoblast cell lines using RNA interference. At 48 h post-transfection, total RNA was isolated and the expression levels of genes associated with myogenesis (*MYOGENIN*, *PAX7* and *SRF*) and *IGF2* regulation (*ZBED6* and *BAHD1*) were quantified by real-time PCR. Effects of gene silencing on cell proliferation and differentiation were also assessed. The alternative splicing of various genes was evaluated in *ZC3H11A*-silenced cells. Whole mount mouse embryo and placenta samples were prepared for immunohistochemistry (IHC) at embryonic days 7.5, 8.5, 10.5, 12.5 and 13.5 to visualize the expression pattern of *ZC3H11A* during mouse embryo development. Results showed that silencing *ZC3H11A* was associated with a down-regulation of *MYOGENIN*, *PAX7* and *BAHD1* mRNA ( $p < 0.05$ ). As silencing of *ZC3H11A* targets the transcript containing *ZBED6*, *ZBED6* mRNA was also down-regulated ( $p < 0.001$ ). When *ZBED6* was knocked down in C2C12 cells using siRNA, *IGF2* mRNA was up-regulated ( $P < 0.001$ ) more than 2-fold. No aberrant RNA splicing was detected in *ZC3H11A*-silenced cells. Immunohistochemical staining revealed a nuclear localization for the *ZC3H11A* protein. The *ZC3H11A* protein was restricted to certain tissues during embryo development, particularly cartilage and muscle. *ZC3H11A* appears to be a factor important for mammalian development. Because of the integration of *ZBED6* into the first intron of the *ZC3H11A* gene and use of a common promoter for transcription, it is difficult to elucidate the underlying mechanisms regarding regulation and function of these two unique genes.

**Key words:** *ZC3H11A*, splicing machinery, myogenesis, *ZBED6*.

## **Introduction:**

Recently, a domesticated transposon and novel transcription factor, *ZBED6*, was discovered within the first intron of *ZC3H11A*, a gene that encodes a poorly characterized zinc finger protein (Markljung et al., 2009). It is estimated that *ZBED6* integrated into the genome of a primitive mammal some 200 million years ago and since that time, lost the ability to transpose, and very importantly from an evolutionary perspective, acquired an essential function. That *ZBED6* gene is unique to placental mammals suggests that integration and maintenance of this gene was important for the evolution of the placenta. Transcription of both *ZC3H11A* and *ZBED6* is initiated from a common promoter and the amount of *ZBED6* and *ZC3H11A* coding sequence is regulated by alternative splicing (figure 3). When *ZBED6* is expressed due to intron retention, the *ZBED6* protein is translated and *ZC3H11A* is not expressed. Alternatively, when the intron containing *ZBED6* is spliced out, *ZC3H11A* coding sequence is then translated into protein, and *ZBED6* is not translated into protein. We hypothesize that *ZC3H11A* may play a role in regulating splicing machinery. In order to fully understand regulation of *ZBED6* expression and function, we must first gain a better understanding of the regulation of *ZC3H11A* transcription, splicing and gain insight into the function of the *ZC3H11A* protein. Furthermore, we hypothesize that *ZC3H11A* plays a role in muscle development since *ZBED6* plays a role in regulating muscle mass through modulating IGF2 promoter activity. Since the transcriptional activity of *ZBED6* and *ZC3H11A* are intertwined through use of a common promoter, it is possible that they are associated with similar biological processes. Alternatively, since expression of *ZBED6* precludes translation of *ZC3H11A* from that transcript and since *ZBED6* may actively play a role in regulation of intron retention leading to reduced expression of *ZC3H11A*, the two genes may have evolved to have very different functions and protein localization patterns.

## **Muscle development:**

The formation of skeletal muscle includes a series of complex biological processes that occur throughout prenatal and postnatal life. Here I will briefly review muscle development in mammals and the mechanisms regulating the formation of muscle fibers, with a focus on the developmental regulation of genes associated with myogenesis.

### **Myogenesis:**

During the early stages of embryonic development, the three germ layers are formed: ectoderm, mesoderm and endoderm, which are the precursors of the specialized tissues in the adult animal. Skeletal muscles originate from the mesoderm layer, which gives rise to the myogenic progenitor cells and other cell types. These myogenic progenitors develop to form mononucleated myoblasts which continue dividing and proliferating to establish a population of myoblasts (Rehfeldt et al., 2000). The first phase of muscle fiber formation begins when the embryonic myoblasts exit the cell cycle and differentiate to form multinucleated cells called primary myotubes (Dunghlisson et al., 1999; Pin et al., 2002) This phase, known as primary myogenesis, takes place between embryonic day 13- 14 in rat and weeks 6-8 in humans. Later on, between weeks 8 – 18 in human (Barbet et al., 1991) and days 17 – 21 in rat (Wigmore et al., 1998), the secondary myogenesis takes place when fetal myoblasts stop dividing and differentiate to form secondary myotubes on the surface of primary myotubes (Duxson et al., 1995), which are used as scaffold. Thereafter, the secondary myotubes elongate and form individual fibers (figure 1). In human and large animals there is a tertiary wave of myogenesis resulting in the formation of tertiary myotubes.

### **Muscle fiber types:**

Skeletal muscle tissues are comprised of different types of muscle fibers at varying proportions. These muscle fibers are classified into three types (I, IIa and IIb) based on the differences in energy metabolism and contractibility properties. Type I fibers are slow twitch fibers and generate ATP from oxidative metabolism. This type of fiber is rich in myoglobin and contains large numbers of mitochondria. The type II fibers are divided into two subtypes, IIa and IIb, both are fast twitch fibers that differ in energy metabolism processes. The type IIa fibers generate ATP from oxidative metabolism while type IIb fibers derive ATP from anaerobic metabolism (Charlotte, 2008). However, the proportions of fiber type in muscles are not fixed and change in response to various factors such as exercise, hormones and age. The relationship between muscle fiber type and obesity has been investigated by Tanner et al. 2002, and they found that in obese individuals there was a high proportion of type IIb fibers and low proportion of type I and IIa fibers. Further, specific fiber types in muscles are correlated to meat quality traits. A high percentage of type I fibers was associated with superior meat quality in terms of increased protein

solubility, higher pH after slaughter and increased redness (Ryu et al., 2008). Consequently, the composition of muscles is important for human health and for animal production traits.

### **Satellite cells:**

Skeletal muscle has the capacity to regenerate and repair damaged myofibers or form new ones as a response to injury, disease or training (Liu et al., 2010). Adult muscle regeneration requires the activation of undifferentiated cells that are located extracellular to muscle fibers and termed satellite cells (Liu et al., 2010). Satellite cells are myoblasts that have not differentiated into myofibers during the first and second waves of myogenesis and remain proliferative (Rehfeldt et al., 2000) and located in close proximity to muscle fibers. Satellite cells are important for muscle growth during the postnatal phase, where the number of muscle fibers is fixed and muscles grow mainly by hypertrophy, i.e. increase in the size of individual myofiber without an increase in myofiber number (Velloso, 2008). This occurs by myonuclear accretion, whereby satellite cells differentiate and fuse to existing myofibers to provide the additional nuclei to support protein synthesis for postnatal muscle growth (Velloso, 2008). Activation of the satellite cells are regulated by genetic factors such as myogenic regulatory factors (MRF), paired box transcription factors (PAX3 and PAX7) and myocyte enhancer factor-2 (MEF2) (Guasconi and Puri, 2009).

### **Genetic factors regulate skeletal muscle development:**

Muscle development occurs prenatally and takes place during primary and secondary myogenesis. Later on, the number of muscles fibers is fixed and the skeletal muscle fibers grow by hypertrophy during the postnatal growth phase (Rehfeldt et al., 1993; Velloso, 2008). Hence, the number of primary myofibers formed prenatally affects the postnatal growth capacity of skeletal muscles (Oksbjerg *et al.*, 2004; Dwyer *et al.*, 1994). Consequently, the factors that influence the prenatal muscle development are important for the improvement of meat-producing animals (Oksbjerg *et al.*, 2004). One of these factors is regulation of genes associated with myogenesis, which play a crucial role in regulating muscle formation (Olson, 1990).

### **Myogenic regulatory factors:**

Myogenic regulatory factors (MRF) is a gene family that includes *myoD*, *MYOGENIN*, *myf-5* and *MRF4*, which are muscle tissue-specific basic helix-loop-helix transcription factors. Each gene plays a crucial role during muscle development (Buckingham et al., 2003). The expression of myoblast determination protein (MyoD) induces fibroblasts to differentiate into myoblasts. It has also been shown that MyoD has the ability to convert other cell lines such as neuroblastoma, adipocyte and liver cell lines into muscle-like cells when MyoD is activated in these cells (Weintraub et al., 1989). Myf-5 gene accomplishes the same

function as MyoD for determining skeletal muscle lineage, thus the muscle develops normally if one of them is absent, while the absence of both MyoD and Myf-5 genes in the embryo results in complete lack of muscle formation (Rudnicki et al., 1993). Both MyoD and myf-5 are expressed in proliferating myoblasts, while *MYOGENIN* is expressed in differentiating cell cultures. *MYOGENIN* induces the myoblasts to differentiate into myotubes, whereas the other MRF proteins do not induce differentiation (Olson, 1993). The high expression of MRF4 in skeletal muscles of postnatal animals suggests that the role of MRF4 may be in maintaining the skeletal muscle fibers (Walters et al., 2000). MRFs may play a role in specification of fiber types since *MYOGENIN* accumulates at high levels in the muscles that have a high proportion of type I fibers, while MyoD accumulation is observed in muscles with a high percentage of fast twitch (type II) fibers (Hughes et al., 1993).

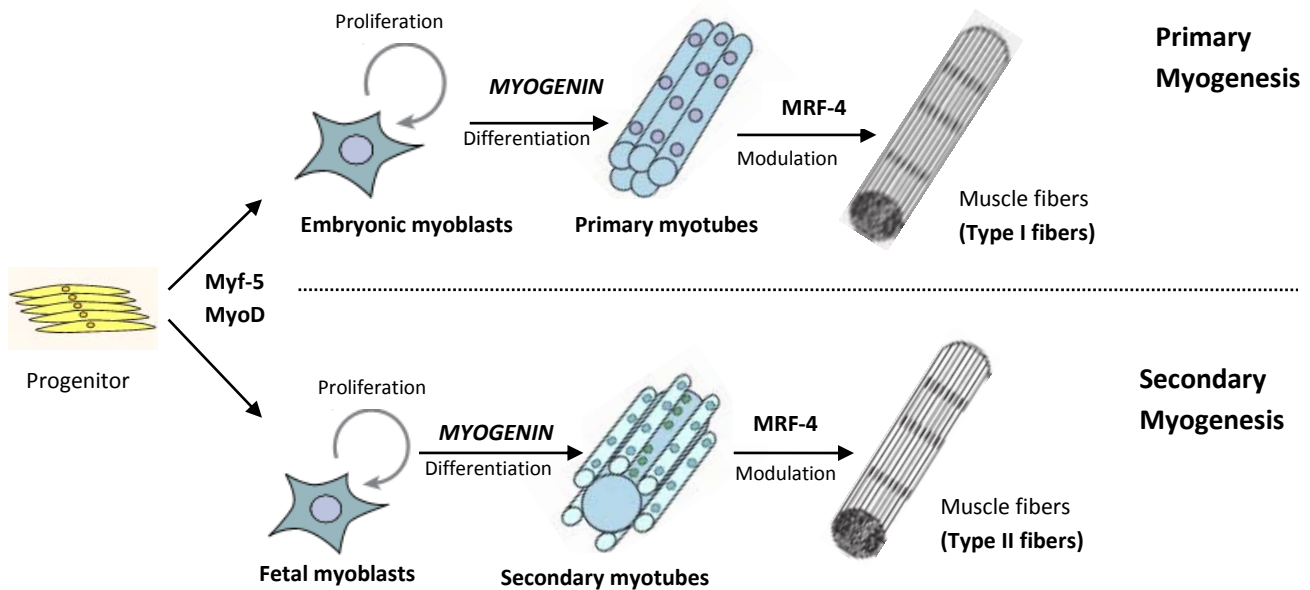


**Figure 1: Basic events of muscle development in mammals.** Cells in the somite are destined to become muscle progenitor cells and then develop into myoblasts through induction by MyoD and/or Myf-5. The myoblasts proliferate to increase the number of fibers. *MYOGENIN* induces the primary myoblasts into differentiation to form primary myotubes. Later, *MYOGENIN* induces the fetal myoblasts to form secondary myotubes on the surface of primary myotubes. Primary myotubes give rise to type I fibers, and secondary myotubes give rise to type II fibers. Based on Buckingham et al., 2007; Pin et al., 2002; Rehfeldt et al., 2000; Dungalsson et al., 1999.

MRF proteins regulate muscle differentiation by interacting with other transcription factors such as E2A proteins, which are also members of the basic helix–loop–helix transcription factor family, to form heterodimers. These heterodimers activate the transcription of muscle-specific genes by binding to the E-boxes of target genes (Olson, 1990). The E-box (5'-CANNTG-3') is a DNA sequence located 5' upstream of genes in the promoter region. On the other hand, the dimerization between MRFs and E2A proteins is regulated by inhibitor of differentiation (Id) proteins (Langlands et al., 1997), which are helix-loop-helix proteins (Sun et al., 2007). The Id proteins dimerize with E2A proteins and form heterodimers that are unable to bind to DNA due to lack of the necessary basic amino acid, and preclude dimerization between MRF and E2A proteins. As a result, muscle-specific genes remain inactivated and differentiation is postponed (Sun et al., 1991).

### **IGFs in muscle development:**

The importance of insulin-like growth factors (IGFs) in muscle development was thoroughly investigated in several studies by both *in vivo* and *in vitro* experiments. The IGFs play a crucial role in both prenatal and postnatal growth. (Oksbjerg et al., 2004). Growth hormone (GH) stimulates the production of IGFs through binding to GH receptors in skeletal muscle tissues, leading to an induction of the local production of IGFs. Hence, it is believed that IGFs can carry out their function in skeletal muscle through autocrine/paracrine mechanisms (Kerr et al., 1990). The IGFs bind the insulin receptor, IGF1-receptor and IGF2-receptor at different affinities. For instance, IGF1 binds IGF1-receptor with relatively higher affinity than IGF2, and binds the IGF2-receptor with 500-fold lower affinity than IGF2 (Jones et al., 1995). The IGFs have been implicated in regulating myoblast proliferation and differentiation. For instance, the expression of IGFs was related to both the proliferation and differentiation of muscle cells. The IGFs are able to induce differentiation by inducing *MYOGENIN* expression (Ernst et al., 1999). Furthermore, IGF2 is important for the transition of myoblasts from proliferation to differentiation (Florini et al., 1991). IGFs regulate both proliferation and differentiation in skeletal muscle through two different intracellular signaling pathways, phosphatidylinositol 3 kinase (PI3K) pathway and mitogen-activated protein kinases (MAPK) pathway. The P13K pathway is involved in cell differentiation while MAPK pathway is involved in cell proliferation as a response to IGF1, whereas most of IGFs function occurs through the IGF1 receptor (Florini et al., 1991). The biological functions of IGFs in myogenesis are modulated by IGF binding proteins (IGFBPs). IGF1 and IGF2 are bound to six types of IGF binding proteins IGFBP1-IGFBP6. The IGFBPs are produced and released by muscle cells during the proliferation and differentiation at different amounts related to IGFs expression level (Hwa et al., 1999), in other word, IGFBPs regulate the amount of IGFs that are available for signaling. *In vivo* studies using knockout mice showed that IGF1 and IGF2 have overlapping functions and can compensate for one another. IGF1-knockout mice showed growth deficiency and IGF2-knockout mice exhibited viable defects

but Double knockout (IGF1 and IGF2) was lethal and resulted in newborn mice with body weights that were 30% of the wild type and huge decreases in the amount of muscle tissues (Liu et al., 1993; Jeh-Ping et al., 1993).

### ZBED6 discovery:

During the last 60 years, consumer preferences have been changed and favored meat with less fat and more muscle. Intense selection for lean pigs resulted in increased muscle mass and decreased subcutaneous fat deposition. Analyses of QTL (quantitative trait loci) in a pedigree developed from an intercross between the European wild Boar and Large White domestic pigs led to identification of a paternally expressed allele at the *IGF2* locus with major phenotypic effects in domestic pigs. Later, a single nucleotide substitution was identified in *IGF2* intron 3 (figure 2) (Van Laere et al., 2003). This causative mutation resulted in 3-fold up-regulation of IGF2 mRNA expression in post-natal skeletal muscle, increasing meat production by 3-4% in domestic pigs. This interesting observation was explained by the discovery of a nuclear protein named ZBED6 (Markljung et al., 2009). In pigs that carry the wild-type QTN (quantitative trait nucleotide) on the paternal allele, this nuclear protein (ZBED6) binds to *IGF2* intron 3 and represses the transcription. In pigs that carry the mutation on the paternal allele, the single nucleotide substitution (G to A) prevents the binding of ZBED6 to QTN site, and consequently *IGF2* mRNA is expressed abundantly (Markljung et al., 2009).

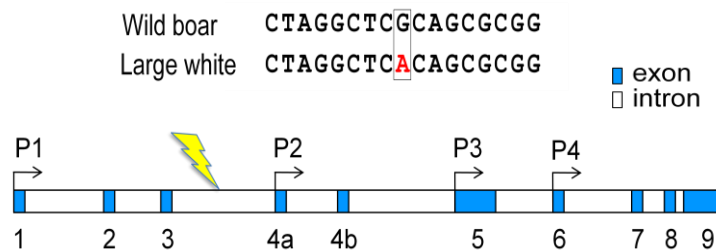


**Figure 2:** The single nucleotide polymorphism (SNP) in *IGF2* intron 3 in pigs

ZBED6 is highly conserved in all placental mammals. The ZBED6 protein contains two zinc finger BED DNA binding domains and a carboxy-terminal hATC dimerization domain, placing it in the hATC (hobo activator tam3) family of DNA transposases. It is encoded by intronless gene located in intron 1 of the *ZC3H11A* gene (figure 3). Both *ZBED6* and *ZC3H11A* are expressed from one promoter located upstream of exon1 of *ZC3H11A*. The amount of translated ZBED6 and ZC3H11A proteins is regulated by alternative splicing. The

ZC3H11A protein is translated in case of proper mRNA splicing, while ZBED6 is expressed due to intron retention. The mechanism of this regulation is not fully clear, but there is a highly conserved intron downstream from *ZBED6* that may also be associated with regulation of *ZC3H11A* transcription (Markljung et al., 2009).

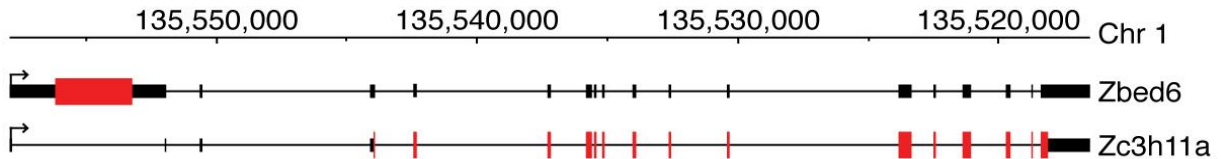


**Figure 3: Genomic structure of *ZC3H11A* and insertion of *ZBED6* in the first intron.** Translated exons are presented in red and untranslated exons are presented in black. (Markljung et al., 2009).

The ZBED6 protein is localized in the nucleolus (Markljung et al., 2009), suggesting that it is involved in processes that occur in the nucleolus such as regulating cell growth and cell differentiation through the tight regulation of ribosomal RNA production and assembly. Furthermore, the promoter region of *ZBED6/ZC3H11A* contains binding sites for the transcription factors Max, Myc, Fos and NF-E2, which are associated with cancer development and are involved in regulating cell proliferation. In addition, according to results of ChIP sequencing experiments performed in mouse myoblast cells, *ZBED6* binds to about 2,500 sites in the genome, many of which are located in regulatory regions of genes relevant to human diseases such as development and neurological disorders, and tumors.

### What is ZC3H11A ?

Zinc finger proteins were first discovered in the middle of the 1980s in the *Xenopus* genome as DNA-binding proteins required to transcribe the 5S ribosomal RNA gene (Miller et al., 1985). A Zinc finger protein contains cysteines and histidines that bind a zinc atom and form zinc finger domains. The “hypothetical” zinc finger facilitates the binding to DNA or RNA. In eukaryotes, zinc finger proteins are quite abundant, comprising approximately 1% of the proteome (Mackay et al., 1998). These proteins are involved in DNA-protein, RNA-protein and protein-protein interactions (Hall, 2005). Zinc finger proteins are classified to belong to different families based on coordination of the zinc atom and finger motifs. In general, there are fourteen different types of zinc fingers. The most common family of zinc finger proteins is Cys2His2, which forms a zinc finger domain through binding of two cysteines and two histidines to a zinc atom (figure 4, A). Cys2His2 proteins mainly bind to

DNA and regulate transcription. They also interact with other proteins and form homodimers or heterodimers (John et al., 2001).

ZC3H11A (Zinc finger CCCH containing 11a) belongs to the CCCH-type zinc finger protein family, which represent about 0.8% of all zinc finger proteins. CCCH-type is constituted by three cysteines (C) and one histidine (H) that bind a zinc atom and form a zinc finger domain (C-X-C-X-C-X-H), where X is any amino acid. Recently, 58, 68, 67 and 55 CCCH-type zinc finger genes were identified in mouse, Arabidopsis, rice and human, respectively (Liang et al., 2008). Most of them are not yet characterized and their functions still unknown (Liang et al., 2008). The CCCH-type zinc finger protein family is classified into six groups based on the copies of the CCCH-type zinc finger motif; the majority of these motifs (79%) are C-X<sub>7-8</sub>-C-X<sub>5</sub>-C-X<sub>3</sub>-H type (Liang et al., 2008). Consequently, *ZC3H11A* is grouped to a subfamily consisting of 9 members, and each one contains three tandem CCCH zinc finger domains (figure 4). Members of the same family or group may have similar biological functions. For instance, Cpsf4 and U2AF1 play important roles in pre-mRNA splicing (Barabino et al., 1997; Justin et al., 2009). Thus, based on a similar putative protein structures, we hypothesized that *ZC3H11A* may also be important in pre-mRNA splicing (figure 4).

Furthermore, there are some CCCH-type proteins that also regulate mRNA stability and play a role in mRNA degradation. For instance, Zfp36, Zfp3611, Zfp3612 and Zfp3613 proteins (also called tristetraprolin (TTP)) increase the rate of turnover of mRNAs containing AU-rich elements (AREs) such as tumor necrosis factor (TNF $\alpha$ ) mRNA. TTP proteins induce mRNA degradation by binding to AU-rich elements in 3' UTRs leading to removal of the poly (A) tail from target mRNAs, and subsequently inducing mRNA degradation (Kramer et al., 2010). Other CCCH proteins are essential for muscle and eye differentiation by regulating mRNA splicing of genes that are important for these processes such as insulin receptor (IR) and muscle-specific chloride channel (ClC-1). The lacking of muscleblind (MBNL) proteins leads to abnormal alternative splicing of these genes (Ho TH. et al., 2004). However, most of the characterized CCCH-type zinc finger proteins bind RNA and carry out different functions including: regulating pre-mRNA splicing (Cpf4, MBNL, U2AF1, U2AF114, ZC3H3 and Zrsr1), controlling RNA stability (Zfp36, Zfp3611, Zfp3612, Zfp3613, Rc3h1, ZC3H2), modification of tRNA (Trmt1) and transcriptional regulation (ZC3H8 and ZC3H12a) (Liang et al., 2008; Kramer. et al., 2010). Many CCCH zinc finger proteins remain uncharacterized. Elucidation of these functions will pave the way for an enhanced understanding of gene regulatory processes.

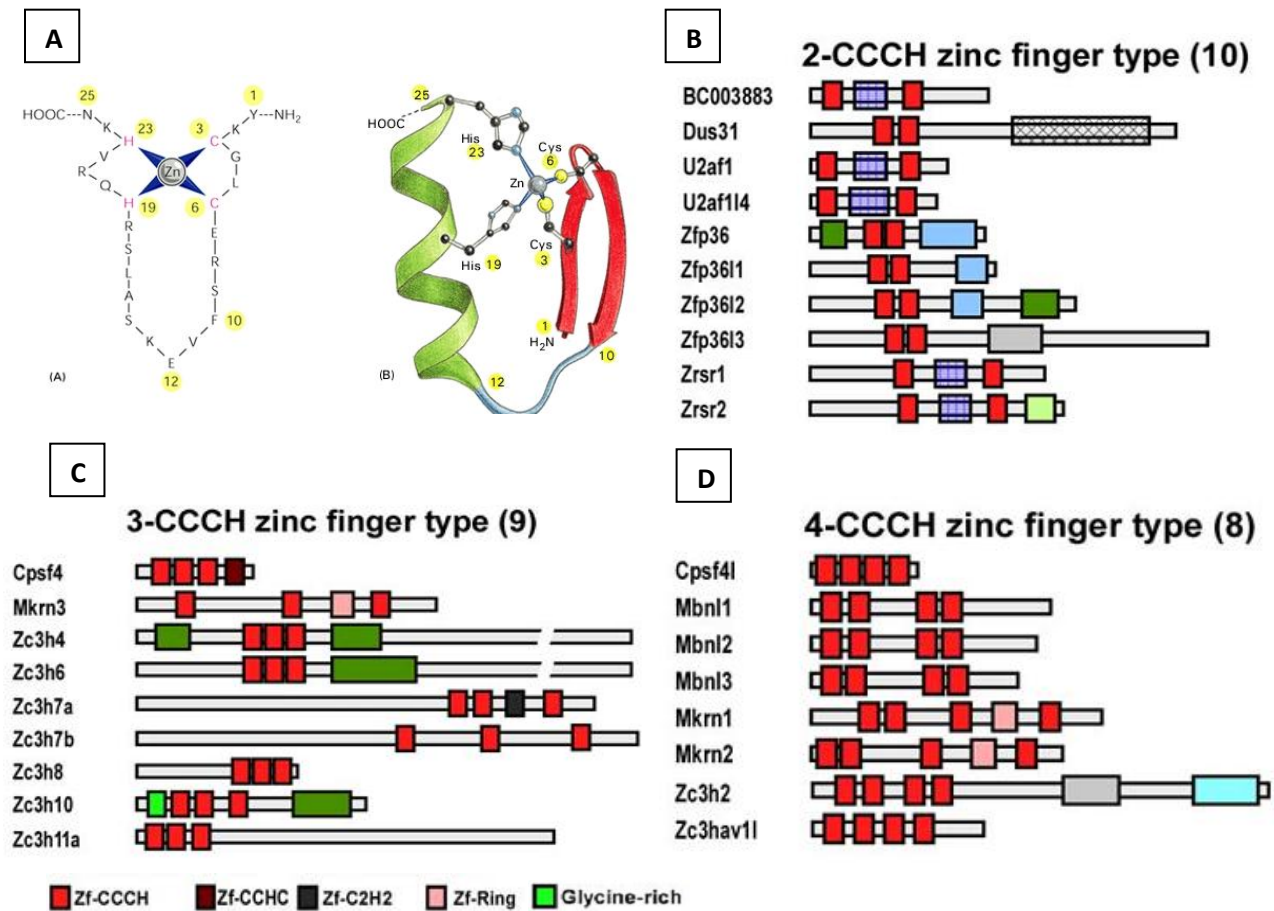


**Figure 4: Structure of zinc finger protein.** A. CCHH-type zinc finger motif, where c=cysteine, h=histidine (Ptashne, 1992); B, C and D. three subfamilies of CCCH-type zinc finger family were identified in mouse genome, and classified base on the number of CCCH zinc finger. Red box represents one copy of CCCH zinc finger, other boxes represent other conserved domains were found in those proteins (Liang et al., 2008).

### Splicing machinery:

Generating a functional protein begins by transcribing the protein-coding gene from DNA into mRNA, followed by mRNA processing i.e. splicing, capping and polyadenylation and then exporting the fully processed mRNA (see below) to the cytoplasm to be translated into a functional protein. Gene transcription in eukaryotes is more complicated than in prokaryotes. In eukaryotic genes, the coding region for a protein is discontinuous and composed of alternating series of coding sequences (exons) and non-coding sequences (introns). Both exons and introns are transcribed from DNA template into pre-mRNA (immature mRNA) even though introns are not needed to synthesize encoded protein. Hence, pre-mRNA requires a maturation process to remove these introns before exporting it to the cytoplasm. This maturation process is called pre-mRNA splicing, in which introns

are excised and remaining exons are ligated together in various patterns (alternative splicing).

The pre-mRNA splicing process is catalyzed by a macromolecular ribonucleoprotein complex called the spliceosome, which is assembled from five small nuclear ribonucleoproteins (snRNPs) and a large number of auxiliary proteins. There are splice sites at the 5' and 3' end of the intron in pre-mRNA. The splice site at the exon/intron junction includes a GU dinucleotide marking the 5' end of the intron. The 3' end of the intron includes three recognition sites: the branch point, polypyrimidine tract and the 3' splice site (AG) (Michael, 1992).

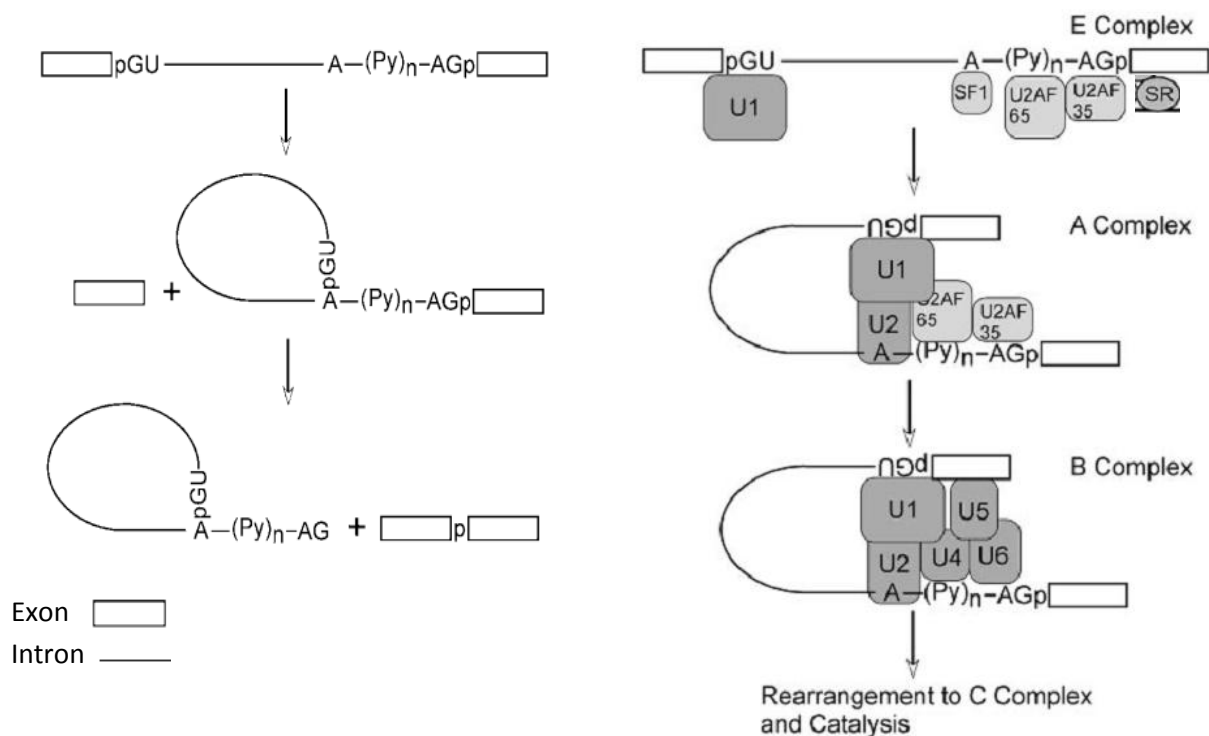


**Figure 5: pre-mRNA splicing mechanism.** (A) Splicing pre-mRNA in two steps. (B) spliceosome complex assembly by U1, U2, U4, U5 and U6 small nuclear ribonucleoproteins (snRNPs) and large number of auxiliary proteins. Michael, 1992.

The splicing reaction takes place in the nucleus and begins when the spliceosome complex assembles on the pre-mRNA. The early complex assembly includes U1snRNP, U2 auxiliary factor (U2AF), splicing factor (SF1) and Serine/arginine-rich proteins (SR). In E-complex, the 5' splice site (GU) is bound by U1 snRNP; SF1 binds to the branch point; the 65 and 35 kDa subunit of the dimeric U2AF attach to polypyrimidine tract and 3' splice site (AG); SR

proteins bind to exonic splicing enhancers (ESEs) (Anireddy, 2007). Thereafter, the A complex is formed when U2 snRNP bind to the branch point, and then the B complex is formed by attaching U4, U5 and U6 tri- snRNP to the A complex (figure 5). Extensive rearrangements occur in B complex including detachment of U1 and U4 snRNP from the complex and binding of U6 snRNP to the 5' splice site instead of U1 snRNP. At this stage the spliceosome is called the C complex, which catalyzes chemical reactions of splicing. The chemical reaction includes cleavage of the 5' exon from the intron and ligation of the intron 5' end to the branch point. The intron is then released from the 3' exon and the two exons are ligated to each other.

Splicing pre-mRNA of a single gene can result in a variety of mature mRNAs giving different proteins. After removing introns from pre-mRNA, the remaining exons ligated to one other in different combinations resulting in different mRNAs (Michael, 1992). This phenomenon is called alternative splicing, and it is this added complexity of gene regulation rather than the total number of genes that distinguishes a more complex organism from a less complex organism. It is estimated that about 60% of human genes undergo alternative splicing. Different patterns of alternative splicing are represented below in figure 6.

Alternative splicing may also occur when the spliceosome does not recognize the correct splice sites, or where some auxiliary elements activate or repress splice sites. For instance, exon splicing enhancers (ESEs) and intron splicing enhancers (ISEs) can activate adjacent splice sites and ESEs contain binding sites for SR proteins, the essential splicing factors that regulate alternative splicing. The exon splicing silencers (ESSs) or intron splicing silencers (ISSs) can repress splice sites or enhancers. The balance of these competing influences determines exon inclusion or skipping (Arianne et al., 2005).

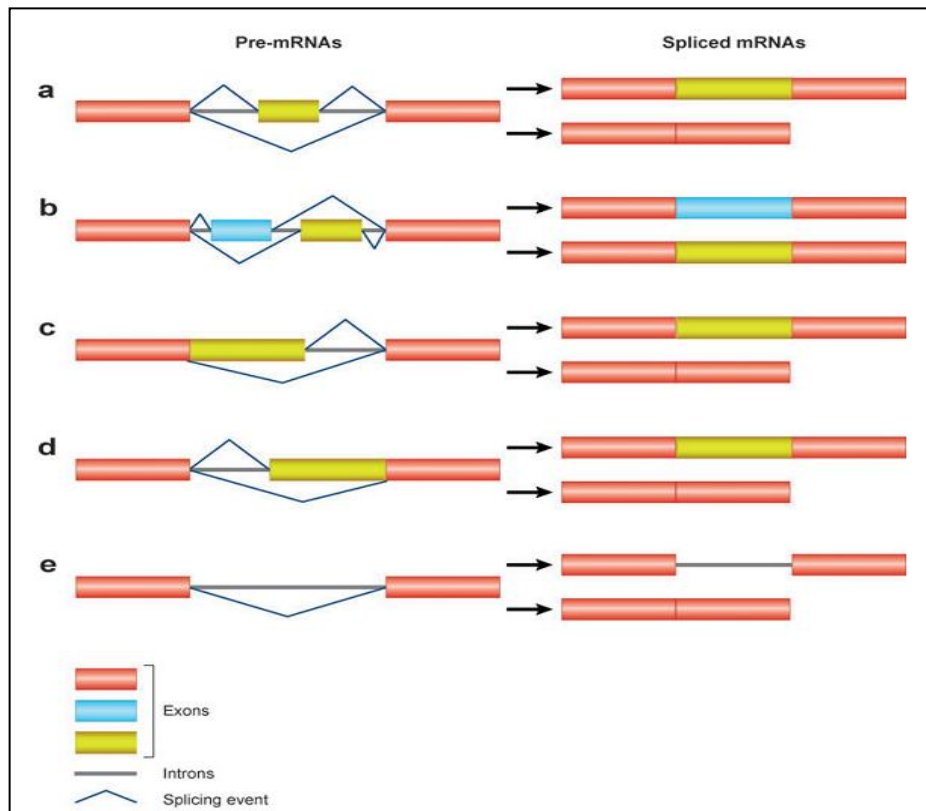


**Figure 6: Alternative splicing patterns.** (A) Cassette exon, which can either be included or excluded from the mRNA; (B) Mutually exclusive splicing, two adjacent exons are spliced and only one exon is included in mRNA; (C, D) Alternative 5' and 3' splice sites allow for mRNA of different sizes depending on the use of proximal or distal splicing sites; (E) Intron retention or excision will result in mRNA with different sizes; Based on Anireddy (2007).

### Aim of thesis:

- Knocking down *ZC3H11A* mRNA in C2C12 cells in order to investigate its effect on the expression of muscle-specific genes, and its influences on cell differentiation.
- To investigate the role of *ZC3H11A* in RNA splicing machinery through evaluating the splice junction of a set of genes.
- To explore the expression pattern of *ZC3H11A* protein during embryo development.

## **Materials and methods**

### **Cell culture:**

Murine myoblast C2C12 cells were originally established from the thigh muscle of mice (D. Yaffe et al. 1977). C2C12 cells are capable of proliferation and differentiation in cell culture (Yoshiko et al. 1996). Therefore, C2C12 cells are widely used as a model system for *in vitro* muscle development, cell proliferation and differentiation.

C2C12 cells at passages less than twenty were cultured in Dulbecco's Modified Eagle Medium (DMEM) supplemented with 10% heat-inactivated fetal bovine serum (FBS; Invitrogen), Penicillin + Streptomycin (0.2 µg/ml) and L-glutamine (0.2 µg/ml) (Invitrogen) in T75 flasks (BD Falcon) at 37°C in a humidified atmosphere of 5% CO<sub>2</sub>. The cultures were split at a ratio of 1:10 to 1:20 every 48 or 72 hours by trypsinization of the cells with 0.25% trypsin (Invitrogen) at 70-80% confluence.

C2C12 cells were induced to differentiate into myotubes at 50-60% confluence by replacing the growth medium with differentiation medium (DMEM supplemented with 2% heat-inactivated horse serum and 0.2 units of antibiotic solution) in gelatin-coated plates followed by changing the medium each 48 hours during the differentiation. Gelatin-coated plates were prepared by incubating 6-well plates with 1 ml of 0.1% gelatin in each well for 4 hours at 37°C. Thereafter, the remaining gelatin solution was aspirated. During the differentiation, digital photos were captured for each well with a Nikon digital camera.

### **Mouse Embryos:**

Breeding experiments were made between 129 and BALB/C mice. Mouse F1 embryos were collected at the embryonic stages: E7.5, E8.5, E10.5, E12.5 and E13.5. Individual embryos and placentas were either submerged immediately in neutral buffered formalin for histological analyses or RNALater for subsequent total RNA isolation.

### **Histology:**

Embryos and placentas were fixed in formalin for 1 hour (e7.5, e8.5, e10.5) or overnight (e12.5 and e13.5), washed in phosphate buffered saline (PBS) and set in 70% ethanol. Embryos and placentas at e7.5, e8.5 and e10.5 were then embedded in molten agarose. All samples were then embedded in paraffin and 5 micron serial sections were made on a microtome. Embryos were oriented longitudinally. Samples were transferred onto poly-L-lysine-coated slides. Slides were dried overnight in a 37°C incubator.

### RNA interference:

The *ZC3H11A* mRNA was silenced in C2C12 cells using small interfering RNA (siRNA). Lipofectamine 2000 reagent (Invitrogen) was used to introduce the siRNA to the cytoplasm of C2C12 cells. Lipofectamine 2000 forms cationic lipid complexes that diffuse across the lipid bilayer membrane of cells. Reduced serum media (Opti-MEM) (Invitrogen) was used to dilute both Lipofectamine 2000 and 3 siRNA oligonucleotides targeted against different regions of the *ZC3H11A* gene (Table 1). The diluted siRNA and the diluted Lipofectamine 2000 were combined at a ratio 1:1 and incubated for 20 min at room temperature. Thereafter, a suspension of  $8 \times 10^4$  C2C12 cells per well of a 12-well plate in antibiotic-free media were combined and seeded with previously prepared siRNA-Lipofectamine solution. Transfected cells were incubated for 48 hours and used in cell differentiation and proliferation experiments or total RNA was isolated from each well to be used in further assays. The experimental unit was defined as the average of the biological triplicates for an independent passage of cells. A scrambled siRNA oligo 2 (ABI) was used as a negative control.

**Table 1:** siRNA oligonucleotides:

Oligonucleotide	Sense	Antisense
ZC3_oligo 1	CACUGUUGCUGUUAGCAAATT	UUUGCUAACAGCAACAGUGGG
ZC3_oligo 2	GAAAGAGCGAGGUCAUAAATT	UUUAUGACCUCGCUCUUUCTT
ZC3_oligo 3	GGAGGUGCAUUAUAAGACATT	UGUCUUAUAUGCACCUCCTG
ZBED_oligo 1	CUUCAACACUUCAACGACAtt	UGUCGUUGAAGUGUUGAAGtt
ZBED_oligo 2	UGUGGUACAUGCAAUCAAAAtt	UUUGAUUGCAUGUACCACAtt
ZBED_oligo 3	GGGCUGUUGCCAACAAAGAtt	UCUUUGUUGGCAACAGCCCaa

### RNA isolation:

Total cellular RNA was isolated from C2C12 cells using the Qiagen RNeasy Mini Kit. First, the media was aspirated from the plates and cells were rinsed with 1ml PBS (Invitrogen). Thereafter, the cells were disrupted by adding 350  $\mu$ L lysis buffer (RLT) to each well. The lysate was homogenized by passing it ten times through a 21 gauge needle and RNA was isolated following the manufacturer's instructions. Genomic DNA contamination was eliminated by following the optional DNase I treatment step in the protocol. Eluted RNA was stored at  $-80^{\circ}\text{C}$ . The quantity and purity of RNA was measured by a NanoDrop® ND-1000 UV-Vis Spectrophotometer at 260/280 nm. RNA integrity was assessed with the RNA 6000 Nano Bioanalyzer chip assay (Agilent).

### Reverse Transcription (RT):

Single stranded RNA was reverse transcribed into complementary DNA (cDNA) using the High Capacity cDNA Archive Kit (Applied Biosystems). Two hundred nanograms of the total RNA was mixed with 2  $\mu\text{L}$  random hexamers, 2  $\mu\text{L}$  RT buffer, 4  $\mu\text{L}$  dNTP (RT) at 2.5 mM, 1  $\mu\text{L}$  reverse transcriptase enzyme and nuclease-free water for a 20  $\mu\text{L}$  total reaction volume. Reverse transcription was performed under the following conditions: 25°C for 10 min, 37°C for 120 min to extend the RT reaction and 85°C for 5 sec to inactivate the enzyme. The cDNA was diluted 8-fold with nuclease-free water to be used in qPCR and stored at -20°C.

### Quantitative PCR (qPCR):

The changes in expression level of mRNA for genes of interest were quantified by Real-time Polymerase Chain Reaction (real-time PCR) using TaqMan® chemistry. With TaqMan PCR, forward and reverse primers are used to amplify the target sequence, and a specific fluorogenic probe binds within the amplicon. These probes are labeled at the 5'-end with a fluorescent reporter dye (6-carboxy-fluorescein (FAM)) and at the 3'-end with a non-fluorescent quencher. When Taq polymerase extends the amplicon, the nuclease activity of polymerase cleaves the fluorophore on the probe, releasing it from the non-fluorescent quencher, and the fluorescence is detected in real time with each cycle of amplification (figure 8). The amount of detected fluorescence is used to quantify the amount of PCR product. For an added degree of specificity, we used probes containing MGB (minor groove binder) on the 3' end. These MGB molecules bind to the minor groove of duplex helical DNA to increase the specificity and stability of the probe during the real-time PCR reaction (Kutyavin et al., 2000).

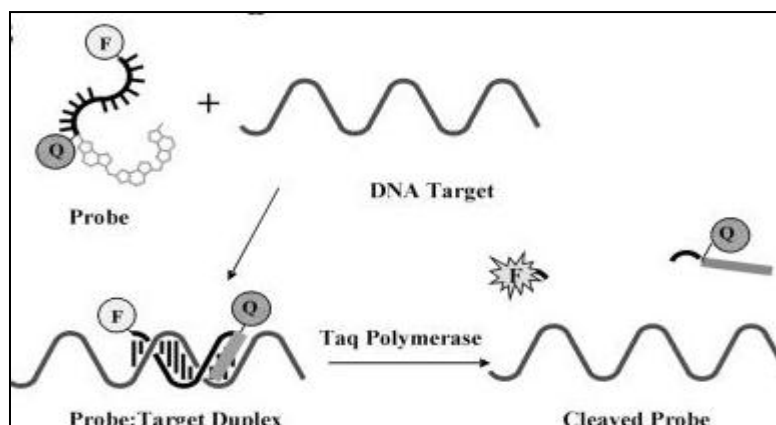


**Figure 8:** The MGB probe binds to the minor groove of target DNA to increase the specificity and stability of the probe. (Kutyavin et al., 2002.)

The following primers and probes were used in this project: **18S rRNA**: forward: 5'-AGTCCCTGCCCTTTGTACACA-3', reverse: 5'-GATCCGAGGGCCTCA CTAAAC-3', probe: 5'-CGCCCGTCGCTACTACCGATTGG-3; **ZBED6**: forward: 5'-CAAGACATCTGCAGTTTGGAAATTT-3', reverse: 5'-TGTCGTTGAAGTGTTGAAGTTCCTA-3', probe: 5'-ACATCTCAAGAGCTGTGTGT-3'; **IGF2**: forward: 5'-CGTGGCATC GTGGAAGAGT-3', reverse: 5'-ACACGTCCCTCTCGGACTTG-3', probe: 5'-CTGGCCCTCCTGGAG -3'; **ZC3H11A**: forward: 5'-TTGTCATCGGTTCCGGTAAAGTTT-3', reverse: 5'-CATCTGTGTCTTCACT CAGTTCCAA-3', probe: 5'-TGTTCTCTGGCGTAATAG-3'; **MYOGENIN**: forward: 5'-GGCTGCCTAAAGTGGAGATCCT-3', reverse: 5'-AGGCCTGTAGG CGCTCAAT-3', probe: 5'-CAGCGCCATCCAGT-3'; **PAX7**: forward: 5'-TCCCGTCAGCTCCGTGTT -3', reverse: 5'-TCCTGATATCGGCACAGAATCTT-3', probe: 5'-CCCATGGTTGTGTCTC; **SRF**: forward : 5'-ACCCACACAGACCAGAGA-3', reverse: 5'-GGTAGGTGAGATCTGGCTCTTCA-3', probe: 5'-TGAGTGCCACTGGCT-3', BAHD1: (Refseq: NM\_001045523): TaqMan® Gene Expression Assay (Applied Biosystems, Mm01279557\_m1). All probes and primers were designed by Primer Express® Software v3. (Applied Biosystems).

Real-time PCR reactions were performed in ABI MicroAmp Optical 384-well Reaction plates with 20µL total reaction volume, each reaction containing 4 µL of diluted cDNA, 250nM probe, 900 nM forward and reverse primers and 1X TaqMan Gene Expression Master Mix (Applied Biosystems). In the case of 18S rRNA and IGF2, 700 nM of forward and reverse primers were used in the PCR reaction. Quantities of primers were determined in an optimization experiment, where the concentration of primers yielding the greatest Rn was evaluated. The following thermal cycler conditions were used for running the PCR reaction on an ABI 7900 real-time PCR instrument: 50°C for 2 min, 95°C for 10 min and 40 cycles of 95°C for 15 sec and 60°C for 1 min (Applied Biosystems 7900 system).

### Data analysis:

Data were analyzed using the relative quantification method ( $2^{-\Delta\Delta CT}$ ), whereby Ct values of the target transcript were normalized to a housekeeping gene (18S rRNA endogenous control) and plotted as fold change in gene expression relative to a calibrator (scrambled siRNA samples)( Kenneth *et al*, 2001).

Primer amplification efficiency was assayed by absolute quantification using a standard curve consisting of 3-fold serial dilutions of cDNA from C2C12 cells subjected to qPCR amplification as described previously. Thereafter, a standard curve was prepared using Ct values of serial dilutions that were plotted against the concentration of cDNA. The efficiency was calculated using this equation  $E = 1 - 10^{(-1/\text{slope})}$ , where slope is the slope of the standard curve. All efficiencies were within 5 % of 100 %, validating the assumption that the efficiencies of the housekeeping genes and target genes are roughly equal and that the amplicon is doubling each cycle.

### PCR to assess the splicing efficiency:

Polymerase chain reaction was performed using the KAPA2G Robust PCR kit (KAPA Biosystems). PCR reactions were carried out in 25  $\mu$ L total reaction volume containing 0.5  $\mu$ L of dNTP Mix (10 mM each dNTP), 5  $\mu$ L of 5X KAPA2G Buffer A, 0.1  $\mu$ L KAPA2G Robust DNA Polymerase (5 units/ $\mu$ L), 3  $\mu$ L of cDNA and 1.5  $\mu$ L each of forward and reverse primer(5pmol)(Table 2). The PCR reaction was performed at the following thermal cycler conditions: 95°C for 3 min for the initial denaturation, followed by 35 cycles of 95°C for 15 sec, 60°C for 20 sec, 72°C for 45 sec and 72°C for 3 min. PCR products were separated by electrophoresis on a 2% agarose gel (SeaKem) at 90 V for 1 hour.

**Table 2:** Primer sequences

Gene	Accession number	Direction	Primer ID	Primer sequence (5' to 3')	Position
<b>MYOGENIN</b>	ENSMUST00000027730	Forward	Myos1	ACCAGGAGCCCCACTTCTAT	Exon
		Forward	Myos2	GGCCACCAGAGCTAGAACAG	Intron
		Reverse	Myo_as3	TGTGGGAGTTGCATTCCTG	Exon
<b>IGF2</b>	ENSMUSG00000048583	Forward	IGF2s1	GGAAGTCGATGTTGGTGCTT	Exon
		Forward	IGF2s2	GTATCCGGCCAGGGTCTAGT	Intron
		Reverse	IGF2_as3	CGTTTGGCCTCTCTGAACTC	Exon
<b>PAX7</b>	ENSMUSG00000028736	Forward	PAX7s1	ACCCACTACCCGGACATCTA	Exon
		Forward	PAX7s2	GCTGGGCAGAGAAACAACCTC	Intron
		Reverse	PAX7_as3	TGACAGGGTTCATGTGGTTG	Exon
<b>SRF</b>	ENSMUST00000015749	Forward	SRFs1	ACGACCTTCAGCAAGAGGAA	Exon
		Forward	SRFs2	CATCTGCTCTCCTCCCTGAG	Intron
		Reverse	SRF_as3	GGTGCCAGGTAGTTGGTGAT	Exon
<b>GAPDH</b>	ENSMUST00000118875	Forward	GAPDHs1	ACTCCACTCACGGCAAATTC	Exon
		Forward	GAPDHs2	CCTTGATATGGTGCAACCTG	Intron
		Reverse	GAPDH_as3	GGATGCAGGGATGATGTTCT	Exon
<b>ZC3H11A</b>	ENSMUST00000027736	Forward	Primer 1	GCAGGAGAGAGGAGCATCAC	Exon
		Forward	Primer 2	ATAGTTCCAGCTGGCCTTGA	Intron
		Reverse	Primer 3	CTTTCTTGGTGGGGCTTTC	Exon

### Immunohistochemistry (IHC):

Dried slides were de-paraffinized and rehydrated by washing with xylene, a graded series of ethanol and PBS. Antigen retrieval was performed by incubating slides in a 0.1 % trypsin (Sigma) solution for 15 min at 37°C. Thereafter, the endogenous peroxidase activities were blocked by incubating the tissues for 15 min in endogenous peroxidase blocking solution (48 ml PBS+ 6 ml methanol +150 ul 30% H<sub>2</sub>O<sub>2</sub>) on ice. Sections were incubated in 10% normal goat serum (NGS, Vector Labs) with 0.1% IPE-GAL in PBS for 13 min to block the non-specific protein binding sites and permeabilize the cell membranes. Thereafter, the

sections were incubated with a solution containing *ZC3H11A* antibody (polyclonal antibody raised in rabbit) at a 1:100 dilution in PBS and 5 % NGS in PBS for 2 h at room temperature in a humidified chamber, followed by three washes in 1X PBS. Normal goat serum was used as a negative control. Horseradish peroxidase (HRP)-conjugated secondary antibody (SuperPicTure kit, Invitrogen) was added to the sections and slides were incubated for 10 min at RT, followed by three washes in PBS. The diaminobenzidine (DAB) chromogen mixture (SuperPicTure kit, Invitrogen) was added to the samples following the manufacturer's instructions. DAB is oxidized by hydrogen peroxide  $H_2O_2$  and forms dark brown insoluble polymers, which mark the localization of the conjugated antibodies as well as the antigens. Sections were counterstained by methyl green, which stain the chromatin of cells. The slides were placed in preheated methyl green stain (60°C) for 5 min. Slides were dehydrated by washing with a graded series of ethanol then xylene, and then mounted by adding one drop of histomount (invitrogen) media and followed by application of a glass coverslip.

### **Statistical analysis:**

The statistical model for gene expression data included the effect of siRNA treatment. The experimental unit was defined as the average of biological triplicates within an experiment (independent passage of cells). The Relative quantification (RQ) values were used for statistical analysis and were transformed to the reciprocal value to reduce heterogeneity of variance and obtain a normal distribution (Andersson, Andersson et al. 2010). Data were analyzed by one-way ANOVA using SigmaPlot 11.0 and Holms Sidak test as a post-hoc test for all comparisons. Significant differences were defined as  $P < 0.05$ .

## Results

### RNA quality and purity:

Real-time PCR requires pure and intact RNA as a starting template to analyze the gene expression accurately. Thus, the isolated RNA was evaluated by the RNA 6000 Nano assay on an Agilent Bioanalyzer. In this assay, total RNA is added to wells of a chip that contain a fluorescent dye, molecular weight calibration markers and gel matrix. Samples are electrophoresed and integrity is assessed based on size distribution of the RNA. The ratio between 18S rRNA and 28S rRNA bands (the most abundant RNA species in a total RNA sample) is the major indicator of RNA integrity. The results showed intact total RNA without notable degradation. All RNA samples had a RNA integrity number (RIN; Agilent) of 9 or greater.

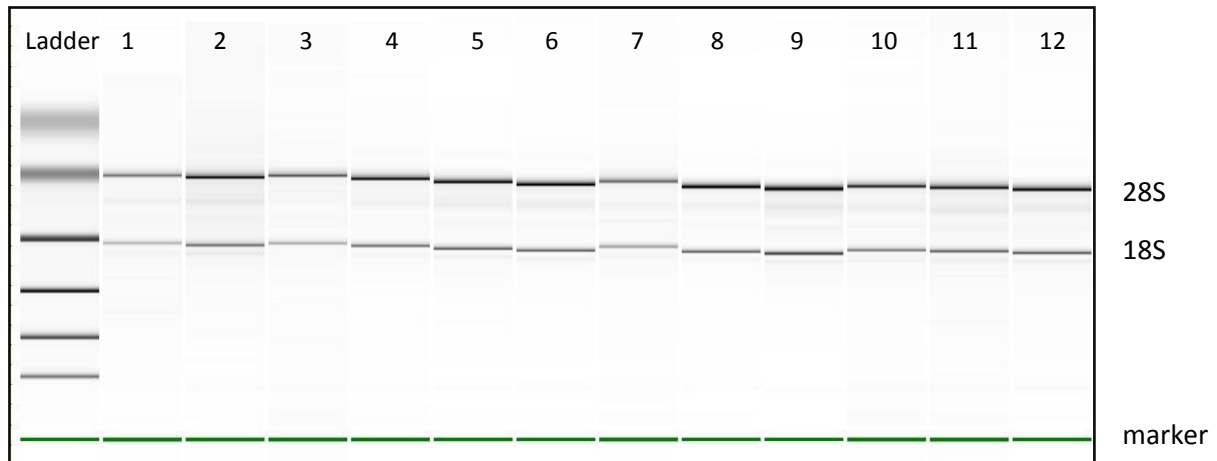


Figure 9: Evaluating RNA quality using RNA 6000 Nano Bioanalyzer.

### The effects of silencing *ZC3H11A* in C2C12 cells:

In order to get further insight into *ZC3H11A* biological function, we silenced *ZC3H11A* in a mouse myoblast cell line by RNA interference (RNAi) to evaluate the effects on the proliferation and differentiation of myoblasts. We Previous study had demonstrated that *ZBED6* plays a major role in regulating muscle development due to its binding to the *IGF2* gene (Markljung et al., 2009). Hence, we were also interested in determining if *ZC3H11A* is involved in similar functions as *ZBED6*. The expression level of number of muscle tissue-specific genes was measured to infer the function of *ZC3H11A* in muscle development. These genes are: *IGF2*, *PAX7*, *SRF*, *MYOGENIN* and *ZBED6*, as they are known for having a functional role in muscle development including myoblast proliferation and differentiation.

In addition, we measured the expression level of BAHD1 to determine if BAHD1 interacts with *ZBED6* or *ZC3H11A*, where BAHD1 binds to the same region of the IGF2 gene as *ZBED6* and has a similar effect on IGF2 expression as *ZBED6* (Bierne et al., 2009).

The siRNA oligonucleotides that target *ZC3H11A*, was expected to also silence *ZBED6* because the *ZBED6* transcript contains the *ZC3H11A* sequence also (figure 3). Hence, it becomes difficult to separate the function of the two transcripts. However, siRNA against the *ZBED6* transcript knocks down only the transcript encoding *ZBED6*. To better separate out the functions of the two genes, I also knocked down *ZBED6* mRNA in each experiment, as described previously.

#### **Most effective siRNA oligo for silencing *ZC3H11A*:**

Three different oligonucleotides of siRNA (Table 1) were used independently at the following three concentrations 12.5, 25 and 50 nM, to find the most effective oligonucleotide concentration for silencing *ZC3H11A*. The real-time PCR was performed 48h after transfection. The results showed that oligonucleotide 2 was the most effective one for knocking down *ZC3H11A* mRNA in C2C12 cells, and there was no significant difference between the three concentrations (Figure 10A). Thus, oligonucleotide 2 was used at the concentration 12.5 nM for silencing *ZC3H11A* mRNA in this project. Data shown in the graph are ( $2^{-\Delta\Delta CT}$ ) values of three biological replicates.

#### **The effect of *ZC3H11A* knock-down on muscle-specific genes:**

The expression level of IGF2, MyoG, PAX7, SRF and *ZBED6* was measured by real-time PCR, at 48 hours after transfecting myoblasts with *ZC3H11A* siRNA. The qPCR data revealed that silencing *ZC3H11A* mRNA resulted in an 80 % down regulation ( $p < 0.001$ ) of *MYOGENIN* mRNA (Figure 10D). As expected, the expression of *ZBED6* mRNA was significantly affected by knocking down *ZC3H11A*, which in parallel down-regulated ( $p < 0.001$ ) as much as *ZC3H11A* mRNA (Figure 10B and C). The *IGF2* mRNA was up-regulated by 40 % after the silencing of *ZC3H11A* (Figure 10). Expression of both PAX7 and BAHD1 mRNAs were reduced ( $P < 0.001$ ) by 60 and 50 percent, respectively, when *ZC3H11A* mRNA was knocked down (Figure 8F and H). Also SRF mRNA was influenced by *ZC3H11A* silencing, and its mRNA was reduced ( $P < 0.05$ ) by 30 percent (Figure 10G).

We repeated the experiment using siRNA oligos targeting the *ZBED6* transcript (Figure 3), and evaluated the effects on the expression of the same set of genes (*ZC3H11A*, *IGF2*, *MYOGENIN*, *PAX7*, *SRF* and *BAHD1*). Myoblast C2C12 cells were transfected with *ZBED6* mouse-specific siRNA oligos (Table 1) at final concentration of 50 nM. Forty eight hours post-transfection, the expression level of genes of interest was measured. Real-time PCR data showed that *ZBED6* mRNA was knocked down ( $p < 0.001$ ) 80 percent (Figure 11, A), approximately the same reduction as when *ZC3H11A* mRNA was targeted. Silencing of

ZED6 mRNA resulted in down-regulation ( $p < 0.01$ ) of *ZC3H11A* mRNA by 60 percent as expected (Figure 11B). Expression of *MYOGENIN* mRNA was affected by silencing *ZBED6* and reduced by about 30 percent. (Figure 11D). Expression of *IGF2* mRNA was up-regulated 2.5-fold ( $p < 0.001$ ) after silencing *ZBED6* mRNA (Figure 11C), a much greater up-regulation than in the case of *ZC3H11A* silencing.

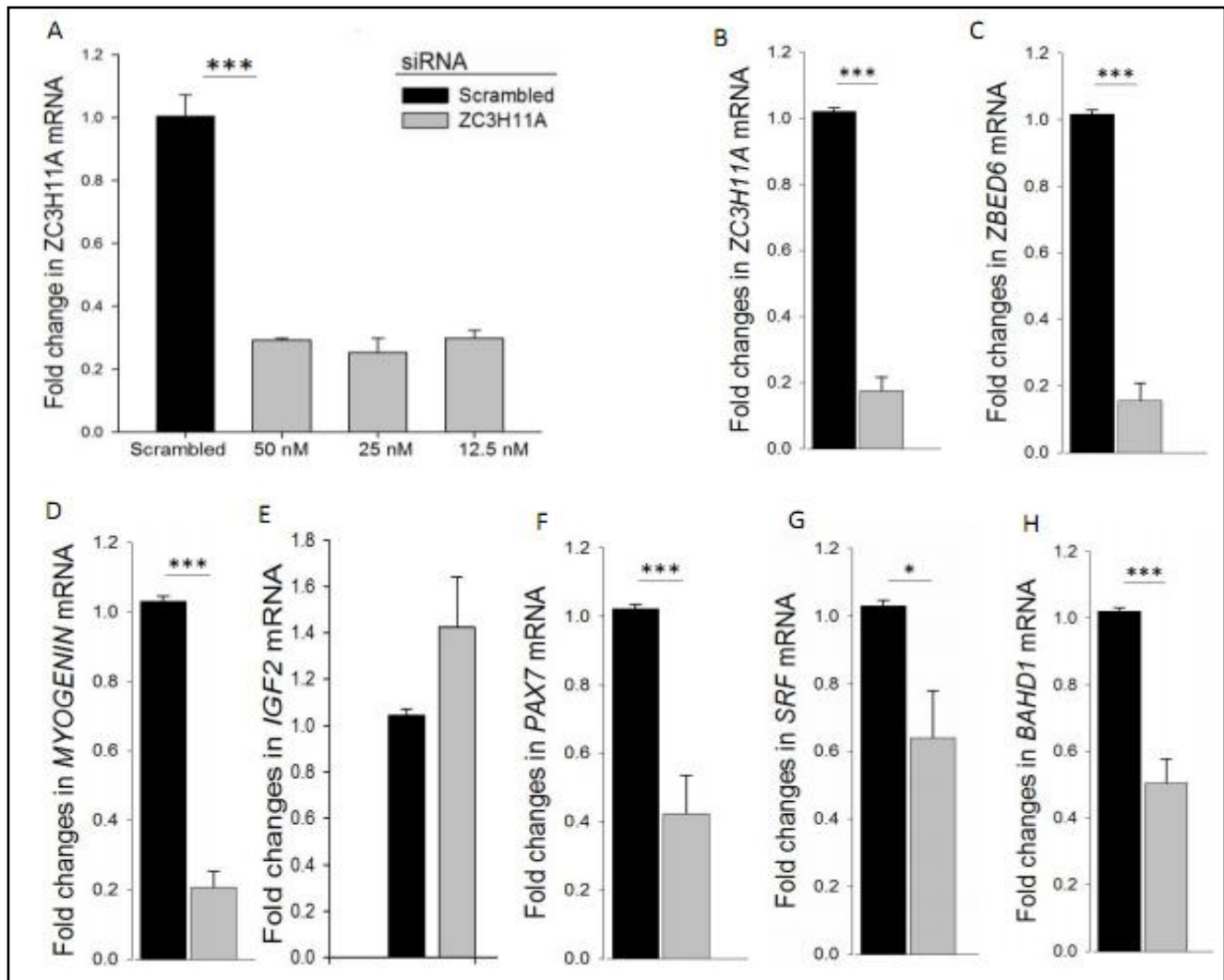


**Figure 10: Silencing *ZC3H11A* in C2C12 cells using siRNA.** A, *ZC3H11A* mRNA expression 48h after targeting it with three different concentrations of oligonucleotide 2. (B-H), The expression level of mRNA for *ZC3H11A*, *ZBED6*, *MYOGENIN*, *IGF2*, *PAX7* *SRF* and *BAHD1* after 48h of silencing *ZC3H11A* with 12.5 nM siRNA oligo 2. Experimental unit N=4. Error bars S.E.M. ( $P < 0.05$ , \*;  $P < 0.01$ , \*\*;  $P < 0.001$ , \*\*\*).

This increase in IGF2 mRNA agrees with previous data (Markljung et al., 2009). Silencing *ZBED6* did not affect *SRF* and *BAHD1* mRNA, whereas *SRF* mRNA was slightly increased and *BAHD1* mRNA was reduced by 15 percent (Figure 11F and G). The *PAX7* mRNA was reduced 40 percent ( $p < 0.001$ ) when *ZBED6* was knocked down (Figure 11E).

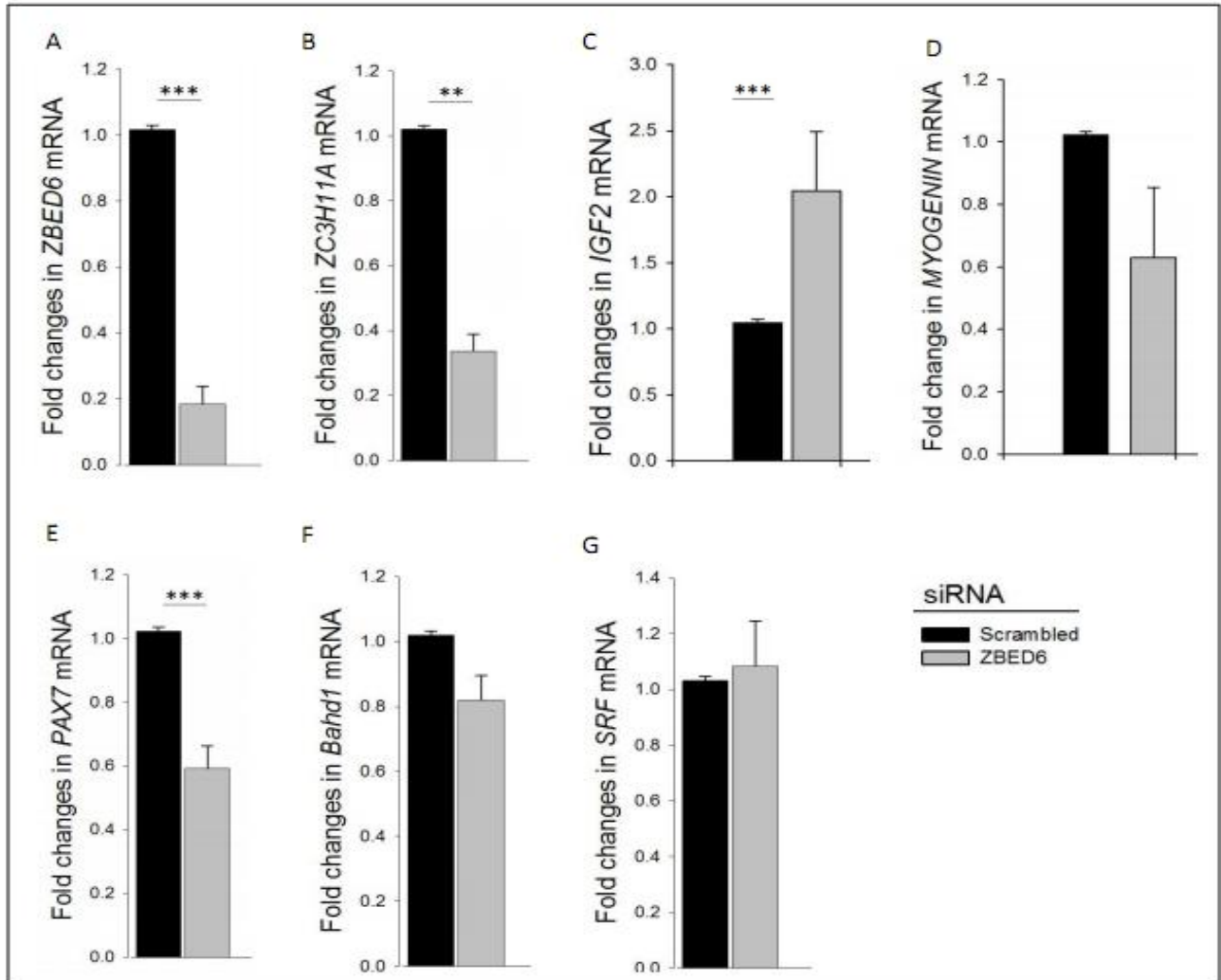


**Figure 11: Silencing *ZBED6* in C2C12 cells using siRNA. (A-G),** The expression level of mRNA for *ZC3H11A*, *ZBED6*, *MYOGENIN*, *IGF2*, *PAX7* *SRF* and *BAHD1* after 48h of silencing *ZBED6* with 50 nM of three siRNA oligonucleotides. Experimental unit N=4. Error bars S.E.M. ( $P < 0.05$ , \*;  $P < 0.01$ , \*\*;  $P < 0.001$ , \*\*\*).

## Does silencing of ZC3H1A affect the differentiation of myoblasts?

Myoblast C2C12 cells were transfected with *ZC3H11A* and *ZBED6* siRNA oligos, independently. Thereafter, the myoblasts were induced to differentiate 48h post-transfection to form myotubes. Morphological changes in differentiating cells were examined under the microscope every 48 h during 6 days, and photographs were taken of each well. The microscopic evaluation did not reveal notable differences between the treatments during the first few days after differentiation was induced. Later, at day 6 of differentiation, there were major differences between the treatment groups. We observed that *ZBED6*-silenced myoblasts formed myotubes faster and more extensively as compared with *ZC3H11A*-silenced myoblasts (Figure 12), while in turn, *ZC3H11A*-silenced myoblasts were differentiating faster than the control group.

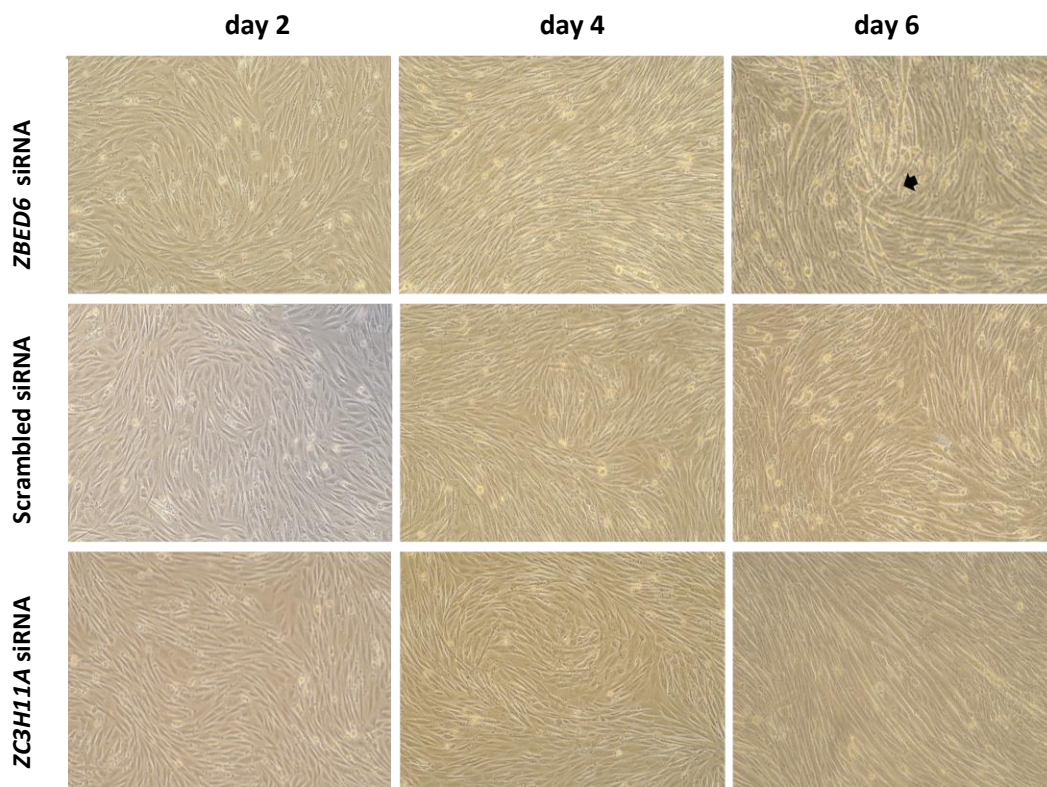


**Figure 12: Microscopic pictures showing the differentiation** at day 2, 4, and 6 of *ZBED6*, scrambled and *ZC3H11A* silenced myoblasts. Differentiation was induced 48 h after transfection with siRNA. Pictures were captured at 10 X, Nikon-TS100 camera. Arrow shows the myotubes.

### Is *ZC3H11A* involved in RNA splicing?

*ZC3H11A* was silenced in C2C12 cells using siRNA and total RNA was isolated. The cDNA generated from RNA was used to evaluate the splice junctions of a number of genes. We hypothesized that if *ZC3H11A* plays a role in splicing machinery, then silencing the gene will have an impact on the splicing of its target genes. The putative target genes included those involved in muscle development as expression of those genes was influenced by silencing of *ZC3H11A*. Three primers were designed for each gene, including one reverse primer on an exon and two forward primers. One forward primer was located in an adjacent exon, and the other forward primer was located in the intron between the exons (figure 13). Two RT-PCR reactions were performed for each gene. The first reaction included primers 1 and 3 that were located in an exon-exon junction to amplify a region that excludes the intron when mRNA is properly spliced, while the second reaction included the same reverse primer plus an intron-located primer (number 2) to give a product that represents unspliced mRNA. These PCR reactions give amplicons with different sizes to discriminate between spliced and unspliced RNA (table 3).

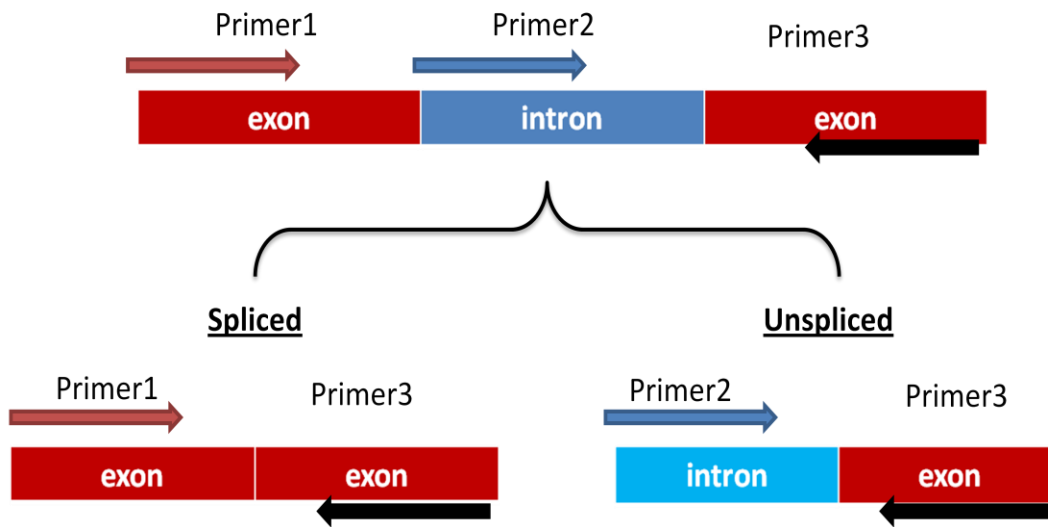


**Figure 13: Primers to evaluate the splice junction using RT-PCR.** Primers 1 and 3 anneal to exonic sequences and amplify a region that excludes the intron when RNA is spliced properly; while primer 2 anneals to intronic sequences. Both primer 2 and 3 amplify the region that includes intron and represent unspliced RNA.

The PCR products of *MYOGENIN*, *IGF2*, *PAX7*, *SRF*, *GAPDH* and *ZC3H11A* were electrophoretically separated on 2 % agarose gels. One single band was detected in each lane corresponding to the RT-PCR reactions including exon-located primers. These bands

were in the size range 400 to 500 bp (Table 3). These fragments reflect the amplification of exonic regions excluding the intron in between; otherwise, the fragment size would be more than 1 kb if the intron was retained (Table 3). On the other hand, the second RT-PCR reaction, represents an unspliced product, did not give any product for any genes. The fragment size was deduced by running a DNA ladder on the gel in parallel with the samples.

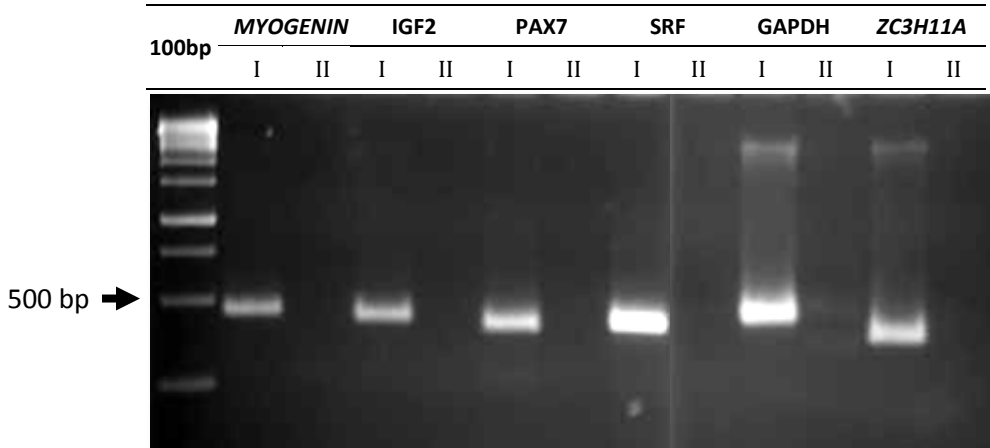


**Figure14: Electrophoretic separation of RT-PCR products to evaluate the splice junction.** Two PCR reactions were performed for each gene. The first one (I) includes an exonic forward primer while the second reaction (II) includes an intronic forward primer. A 100bp DNA ladder was used to detect the fragment size.

**Table 3:** The anticipated DNA fragment size from each PCR reaction.

Gene	Spliced properly		Non-spliced		Results
	I	II	I	II	
<i>MYOGENIN</i>	465	-	995	530	Spliced
<i>IGF2</i>	445	-	1670	696	Spliced
<i>PAX7</i>	421	-	4100	652	Spliced
<i>SRF</i>	440	-	4068	667	Spliced
<i>GAPDH</i>	482	-	714	502	Spliced
<i>ZC3H11A</i>	404	-	1736	615	Spliced

### **ZC3H11A cellular localization:**

It is important to evaluate the expression pattern of a protein of interest and determine its cellular localization to determine the cellular function of this protein. In order to characterize ZC3H11A protein, we stained murine tissues that were obtained from embryos at different embryonic stages. The Immunohistochemistry (IHC) was performed to visualize the expression pattern of ZC3H11A protein in the tissues and organs, as well as its cellular localization. IHC data showed strong staining for ZC3H11A protein in cell nucleus and less staining in cytoplasm (Figure 15). Dark brown color represents that the protein is present.

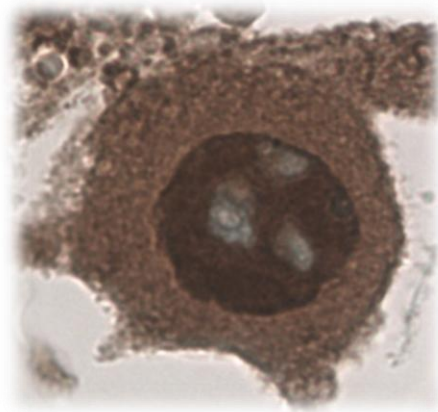


**Figure 15: Cellular localization of ZC3H11A protein.** Embryonic cell obtained from mouse embryo at E8.5. Dark brown shows the expression of ZC3H11A protein in cell nucleus. Green spots are Methyl Green counterstaining

## ZC3H11A protein expression pattern during embryo development:

### Chest and Back:

Immunohistochemistry (IHC) staining for ZC3H11A protein in mouse embryo at embryonic day 13.5. There was intense staining for ZC3H11A in cartilage tissues of humerus, ribs and vertebrae, as well as in skeletal muscles around the neural tube (Figure 16).

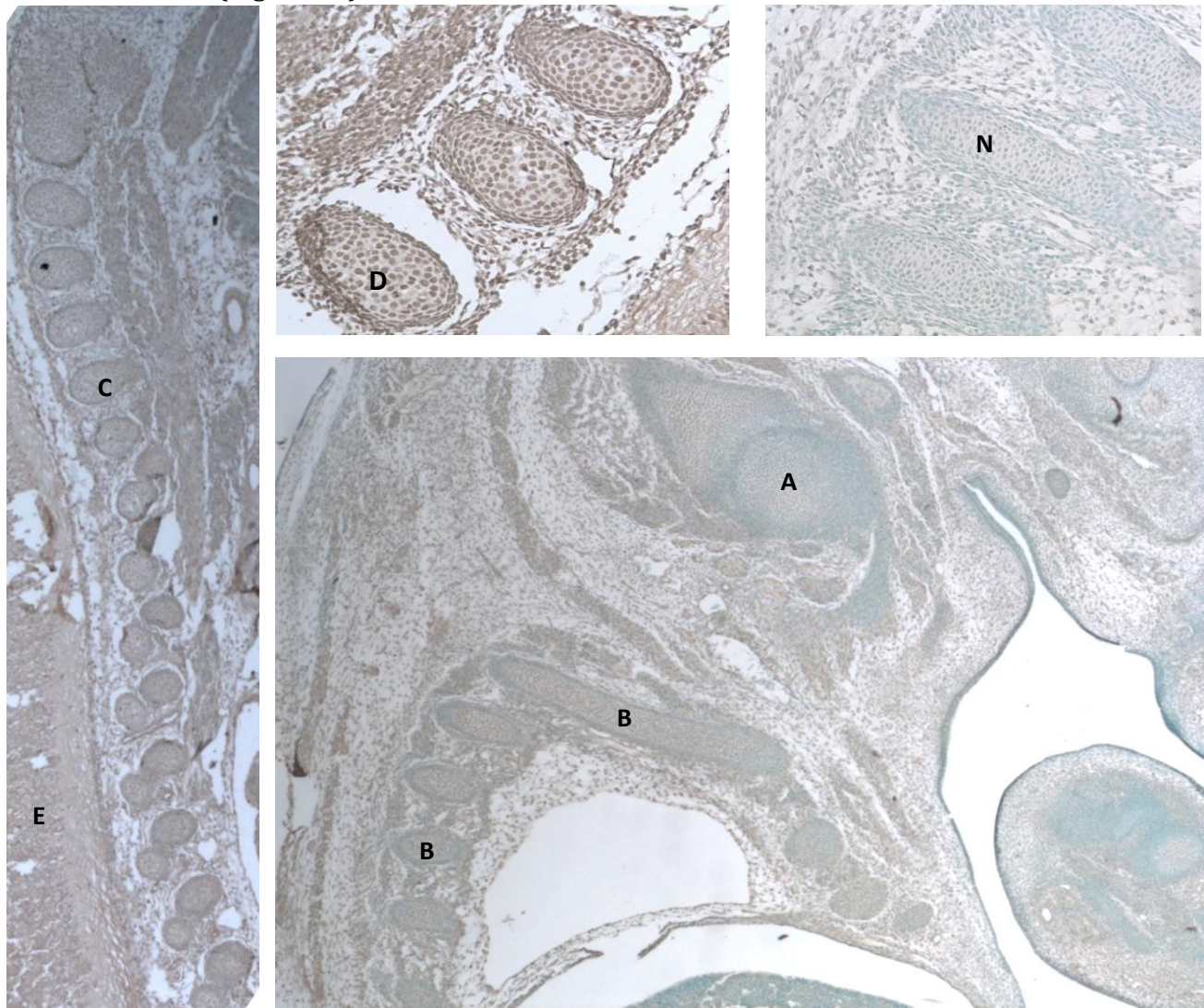
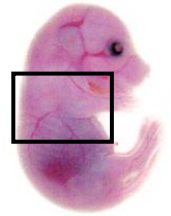


**Figure 16: Localization of ZC3H11A proteins in a mouse embryo at embryonic day 13.5.** Longitudinally section of embryo at low magnification (10X). **A:** Cartilage of primordium of proximal part of shaft of humerus, **B:** Cartilage primordium of second and fifth ribs. **C:** Cartilage primordium of vertebra (10x). **D:** Cartilage primordium of vertebra (20X). **E:** Muscles around neural tube. **N:** Negative control to the same region shown in D. Based on M. H. Kaufman, 1992.

## Discussion:

ZC3H11A is a poorly characterized zinc finger protein that belongs to the CCCH- type zinc finger family with 58 known members in mouse, most of them still uncharacterized (Andersson et al., 2010). ZC3H11A protein contains in its structure three tandem CCCH-zinc finger domains. Members of this family are identified as RNA-binding protein where zinc finger domains facilitate direct binding to mRNA. For instance, U2AF1 and Cpf4 are essential for regulating pre-mRNA splicing. Other proteins in this family increase the rate of mRNA turnover by removing the poly A tail from mRNAs that contain AU-rich elements (Liang et al., 2008). The molecular function of ZC3H11A was investigated using RNA interference. Silencing or reducing the normal level of a gene of interest can provide information about function through the evaluation of effects of silencing on other parameters such as morphological changes in cell culture and changes in expression patterns of other genes. In this project, we silenced *ZC3H11A* in a mouse myoblast cell line using small interfering RNA. Thereafter, the expression levels of mRNAs of interest were analyzed by real-time PCR to explore the influence of *ZC3H11A* transcript levels on abundance of mRNA for other genes. Afterwards, the proliferation and differentiation rate of myoblasts were assessed 48 h after the transfection with mouse *ZC3H11A*-specific siRNA oligonucleotides. In addition, the splice junctions of putative target genes were evaluated by reverse transcription PCR including primers that were designed for specific locations close to splice junction sites (Figure13). Furthermore, we used immunohistochemistry (IHC) to determine the localization of *ZC3H11A* during embryonic development.

Silencing of ZC3H11A was accompanied by an equivalent down regulation of *ZBED6* mRNA (Figure 10B and C). This observation is explained by the insertion of *ZBED6* in the intron number 1 of *ZC3H11A* gene (Figure 3; Markljung et al., 2009). Both *ZC3H11A* and *ZBED6* have the same pre-mRNA, if this pre-mRNA is spliced normally, ZC3H11A protein would be expressed. The *ZBED6* mRNA is expressed in the case of retention of intron 1. Thus, targeting *ZC3H11A* mRNA with siRNA oligonucleotides resulted in down regulation of both ZC3H11A and ZBED6. However, the expression pattern of some muscle development-related genes such as *MYOGENIN* and *IGF2* were affected differently in both cases of silencing. We observed a 4-fold reduction in *MYOGENIN* mRNA expression as a response to silencing *ZC3H11A*, whereas the reduction in *MYOGENIN* mRNA was not significant when only *ZBED6* was silenced (Figure10D). This observation reflects a possible role for ZC3H11A in regulating the expression of *MYOGENIN* in skeletal muscle. The *IGF2* mRNA was increased significantly when *ZBED6* was silenced but to a lesser extent when *ZC3H11A* was knocked down (Figure 10C and E). Those two observations raise the question about the relationship between ZC3H11A and muscle development. However, we are unable to exclude the possibility that the effect of ZC3H11A is a generalized response, limited not only to muscle-related genes. The lack of a negative effect of ZC3H11A silencing on *IGF2*

expression may have been compensated for by the fact that knocking down only *ZBED6* mRNA results in more than a 2-fold increase in *IGF2* expression.

The myoblasts formed myotubes when differentiation was induced even though *MYOGENIN* was down-regulated. The low level of *MYOGENIN* might be compensated for by an up-regulation of *IGF2* when *ZBED6* is knocked down. It may also be that low levels of *MYOGENIN* are sufficient for inducing muscle cell differentiation. As Olsson (1993) has mentioned, IGFs are able to stimulate proliferation and differentiation in different cell types. Consequently, the difference in differentiation rate between *ZBED6*-silenced cells in comparison with *ZC3H11A*-silenced cells could be due to two factors: first, significant reduction in *MYOGENIN* mRNA in the case of *ZC3H11A* silencing, and the second factor might be the up-regulation of *IGF2* in the case of *ZBED6* silencing. Those two factors resulted in notably faster differentiation rate in *ZBED6*-silenced cells with a greater number of myotubes (Figure 12).

We also investigated the possible function of *ZC3H11A* in pre-mRNA splicing, since a number of CCCH-domains bind RNA or are present in proteins that are involved in metabolism or processing of RNA (Liang et al., 2008). Evaluating the splice junction of a number of genes showed that *ZC3H11A* most likely does not affect splicing. However, we cannot draw a definitive conclusion from this experiment since *ZC3H11A* was not knocked down completely. According to real-time PCR results (Figure 10B) there was 80% down-regulation in *ZC3H11A* after 48 hours of silencing with siRNA. A remaining *ZC3H11A* protein may be sufficient for its biological functions. Functional redundancy is a recurring theme in nature. There may also be other genes that have a similar function and compensate when *ZC3H11A* is knocked down. The reason for incomplete knockdown of *ZC3H11A* could in part be due to a lack of complete mRNA degradation as well as residual protein remaining at the time of transfection with siRNA. If *ZC3H11A* or *ZBED6* are long-lived proteins, there may need to be a longer window of time between transfection and analysis of cellular function. Actually, we performed Western blot 48 h after transfection and we found that *ZC3H11A* proteins still could be detected in the cells.

Furthermore, we only evaluated a single splice junction for each putative target gene. We chose the splice junction closest to the 3' end of the mRNA, since oligo dT primers were used for the reverse transcription reaction. It is possible that other splice junctions were affected or that the genes we evaluated are not affected by *ZC3H11A*. It would be more ideal to perform a global analysis of pre mRNA splicing to pull out the genes that are potentially affected by *ZC3H11A* down-regulation. To evaluate effects of *ZC3H11A* on splicing of target genes and of effects on splicing of the *ZC3H11A* gene, a northern blot analysis could be used to reveal differential abundance of presence of alternative transcripts.

Immunohistochemistry staining revealed intense staining for ZC3H11A protein in the cell nucleus (Figure 15). Many essential biological processes such as DNA replication, DNA repair, gene transcription, and RNA processing occur in the nucleus. Moreover, analyzing the expression pattern in embryonic tissues illustrated that ZC3H11A is expressed in specific tissues at restricted zones during embryonic development (Figure 14). The ZC3H11A protein was stained intensely in cartilage and muscles tissues (Figure 14), which reveals an important role for ZC3H11A in these cells. We do not know whether ZC3H11A expressed in these cells functions as a splice factor or regulatory factor or both? However, in both cases it appears to be needed at abundant levels. These observations open the door to investigate the real function of ZC3H11A during development, and to determine if ZC3H11A is involved in development of human diseases. *ZC3H11A*-knockout mice may be the next step for addressing these questions.

It is difficult to determine the real function of ZC3H11A by RNAi as both *ZC3H11A* and *ZBED6* are knocked down when cells are transfected with siRNA against the *ZC3H11A*. Thus, it would be more accurate and clear if we used animal model lacking *ZBED6* such as chicken or zebrafish. Indeed, we tried to knock out *ZC3H11A* in zebrafish embryos using standard dose of Morpholino but the treatments were lethal (unpublished). We do not know if it was due to knocking out *ZC3H11A* or to the Morpholino itself. However, we can perform siRNA in chicken muscles since *ZBED6* does not exist in chicken and myoblasts are easily isolated and cultured. Alternatively, using mouse gene knockout for *ZBED6* or *ZC3H11A* will show the pivotal function of these genes in the development, transcription regulation and help us to understand how ZC3H11A and ZBED6 regulate their expression. Does ZBED6 act as regulator factor for its host gene?

We could also use a technique that targets the ZC3H11A or ZBED6 at the protein level where we can clearly knock down one or the other without the complication associated with trying to knock them down at the RNA level.

Other approaches that can be used to explore ZC3H11A function in splicing is investigating if there is interaction between ZC3H11A and an essential splicing factor such as U2 small nuclear ribonucleoprotein auxiliary factor (U2AF) using yeast two-hybrid protein-protein interactions or performing immunoprecipitations followed by mass spectrometry (Zhang et al.,1992).

**Conclusion:**

Studying the molecular function of ZC3H11A suggested that ZC3H11A is involved in the regulation of many genes in myoblasts and is expressed as early as embryo day 7.5 in embryos and placenta, with expression restricted to certain zones of cells throughout development. Knocking down the expression of *ZC3H11A* was associated with significant changes in other genes, muscle-specific genes, suggesting that ZC3H11A is a regulatory factor for these genes. Because structural features of the primary protein structure place ZC3H11A in a family of proteins that associate with splicing machinery, it is possible that ZC3H11A regulates genes as a splicing factor. Nuclear localization for ZC3H11A reveals a possible role for ZC3H11A in gene regulation or RNA processing. However, more studies are needed to clarify the real function of ZC3H11A in biological processes and to explain how the expression of *ZC3H11A* and *ZBED6* are regulated.

## **Acknowledgments:**

I would like to thank all the people that contributed with their expertise and work to the realization of this research through the European Master in Animal Breeding and Genetics (EM-ABG, 2009- 2011), supported by Erasmus Mundus. My special thanks go to Prof. Johann Sölkner and Dr. Gabor Meszaros for providing all kinds of help and support during the course of EM-ABG at BOKU, Vienna.

I am thankful to faculty and staff of SLU for providing kind support throughout the second year of my MSc in Sweden, especially my supervisor Prof. Göran Andersson, and Dr. Birgitta Malmfors, the co-ordinator at SLU.

I would also like to thank IMBIM staff at Faculty of Medicine, Uppsala University, especially Prof. Leif Andersson, Dr. Elizabeth Ruth Gilbert and Dr. Göran Hjälms for their great help during the whole academic year (MSc, 2010-2011).

I would also like to thank all EM-ABG co-ordinators, who have been so helpful and willing to take some time to help place me on the right path.

## References:

- Andersson, L., G. Andersson, et al. (2010). ZBED6: The birth of a new transcription factor in the common ancestor of placental mammals. *Transcription* **1**(3): 144-148.
- Barabino, S. M., W. Hubner, et al. (1997). The 30-kD subunit of mammalian cleavage and polyadenylation specificity factor and its yeast homolog are RNA-binding zinc finger proteins. *Genes & development* **11**(13): 1703-1716.
- Barbet, J. P., L. E. Thornell, et al. (1991). Immunocytochemical characterisation of two generations of fibers during the development of the human quadriceps muscle. *Mechanisms of development* **35**(1): 3-11.
- Bierne, H., T. N. Tham, et al. (2009). Human BAHD1 promotes heterochromatic gene silencing. *Proceedings of the National Academy of Sciences of the United States of America* **106**(33): 13826-13831.
- Buckingham, M., L. Bajard, et al. (2003). The formation of skeletal muscle: from somite to limb. *Journal of anatomy* **202**(1): 59-68.
- Buckingham, M. and F. Relaix (2007). The role of Pax genes in the development of tissues and organs: Pax3 and Pax7 regulate muscle progenitor cell functions. *Annual review of cell and developmental biology* **23**: 645-673.
- Dunglison, G. F., P. J. Scotting, et al. (1999). Rat embryonic myoblasts are restricted to forming primary fibres while later myogenic populations are pluripotent. *Mechanisms of development* **87**(1-2): 11-19.
- Duxson, M. J. and P. W. Sheard (1995). Formation of new myotubes occurs exclusively at the multiple innervation zones of an embryonic large muscle. *Developmental dynamics : an official publication of the American Association of Anatomists* **204**(4): 391-405.
- Dwyer, C.M., Stickland, N.C. and Fletcher, J.M. (1994). The influence of maternal nutrition on muscle fibre number development in the porcine fetus and on subsequent postnatal growth. *Journal of Animal Science* **72**, 911–917.
- Florini, J. R., K. A. Magri, et al. (1991). Spontaneous differentiation of skeletal myoblasts is dependent upon autocrine secretion of insulin-like growth factor-II. *The Journal of biological chemistry* **266**(24): 15917-15923.
- Guasconi, V. and P. L. Puri (2009). Chromatin: the interface between extrinsic cues and the epigenetic regulation of muscle regeneration. *Trends in cell biology* **19**(6): 286-294.
- Hall, T. M. (2005). Multiple modes of RNA recognition by zinc finger proteins. *Current opinion in structural biology* **15**(3): 367-373.
- Hughes, S. M., J. M. Taylor, et al. (1993). Selective accumulation of MyoD and myogenin mRNAs in fast and slow adult skeletal muscle is controlled by innervation and hormones. *Development* **118**(4): 1137-1147.
- Hwa, V., Y. Oh, et al. (1999). Insulin-like growth factor binding proteins: a proposed superfamily. *Acta paediatrica* **88**(428): 37-45.
- Jones, J. I. and D. R. Clemmons (1995). Insulin-like growth factors and their binding proteins: biological actions. *Endocrine reviews* **16**(1): 3-34.

- Kerr, D. E., B. Laarveld, et al. (1990). Effects of passive immunization of growing guinea-pigs with an insulin-like growth factor-I monoclonal antibody. *The Journal of endocrinology* **124**(3): 403-415.
- Kenneth J. Livak, T. D. Schmittgen. (2001). Analysis of Relative Gene Expression Data Using RealTime Quantitative PCR and the  $2^{-\Delta\Delta CT}$  Method. *METHODS* **25**, 402–408.
- Kramer, S., N. C. Kimblin, et al. (2010). Genome-wide in silico screen for CCCH-type zinc finger proteins of *Trypanosoma brucei*, *Trypanosoma cruzi* and *Leishmania major*. *BMC genomics* **11**: 283.
- Kutyavin, I. V., I. A. Afonina, et al. (2000). 3'-minor groove binder-DNA probes increase sequence specificity at PCR extension temperatures. *Nucleic acids research* **28**(2): 655-661.
- Kutyavin, I. V., S. G. Lokhov, et al. (2002). Reduced aggregation and improved specificity of G-rich oligodeoxyribonucleotides containing pyrazolo[3,4-d]pyrimidine guanine bases. *Nucleic acids research* **30**(22): 4952-4959.
- Laity, J. H., B. M. Lee, et al. (2001). Zinc finger proteins: new insights into structural and functional diversity. *Current opinion in structural biology* **11**(1): 39-46.
- Langlands, K., X. Yin, et al. (1997). Differential interactions of Id proteins with basic-helix-loop-helix transcription factors. *The Journal of biological chemistry* **272**(32): 19785-19793.
- Liang, J., W. Song, et al. (2008). Genome-wide survey and expression profiling of CCCH-zinc finger family reveals a functional module in macrophage activation. *PloS one* **3**(8): e2880.
- Liu, H., S. E. Chen, et al. (2010). TIMP3: a physiological regulator of adult myogenesis. *Journal of cell science* **123**(Pt 17): 2914-2921.
- Liu, J. P., J. Baker, et al. (1993). Mice carrying null mutations of the genes encoding insulin-like growth factor I (Igf-1) and type 1 IGF receptor (Igf1r). *Cell* **75**(1): 59-72.
- Mackay, J. P. and M. Crossley (1998). Zinc fingers are sticking together. *Trends in biochemical sciences* **23**(1): 1-4.
- Maltin, C. A. (2008). Muscle development and obesity: Is there a relationship? *Organogenesis* **4**(3): 158-169.
- Markljung, E., L. Jiang, et al. (2009). ZBED6, a novel transcription factor derived from a domesticated DNA transposon regulates IGF2 expression and muscle growth. *PLoS biology* **7**(12): e1000256.
- Mascarello, F., M. L. Stecchini, et al. (1992). Tertiary myotubes in postnatal growing pig muscle detected by their myosin isoform composition. *Journal of animal science* **70**(6): 1806-1813.
- Matlin, A. J., F. Clark, et al. (2005). Understanding alternative splicing: towards a cellular code. *Nature reviews. Molecular cell biology* **6**(5): 386-398.
- McKeown, M. (1992). Alternative mRNA splicing. *Annual review of cell biology* **8**: 133-155.
- Miller, J., A. D. McLachlan, et al. (1985). Repetitive zinc-binding domains in the protein transcription factor IIIA from *Xenopus* oocytes. *The EMBO journal* **4**(6): 1609-1614.
- Morgan, J. E. and T. A. Partridge (2003). Muscle satellite cells. *The international journal of biochemistry & cell biology* **35**(8): 1151-1156.

- Oksbjerg, N., F. Gondret, et al. (2004). Basic principles of muscle development and growth in meat-producing mammals as affected by the insulin-like growth factor (IGF) system. *Domestic animal endocrinology* **27**(3): 219-240.
- Olson, E. N. (1990). MyoD family: a paradigm for development? *Genes & development* **4**(9): 1454-1461.
- Olson, E. N. (1993). Signal transduction pathways that regulate skeletal muscle gene expression. *Molecular endocrinology* **7**(11): 1369-1378.
- Pin, C. L., A. W. Hryciyshyn, et al. (2002). Embryonic and fetal rat myoblasts form different muscle fiber types in an ectopic in vivo environment. *Developmental dynamics : an official publication of the American Association of Anatomists* **224**(3): 253-266.
- Prigge, J. R., S. V. Iverson, et al. (2009). Interactome for auxiliary splicing factor U2AF(65) suggests diverse roles. *Biochimica et biophysica acta* **1789**(6-8): 487-492.
- Ptashne, M. A. (1992) *Genetic Switch*, 2nd ed. Cambridge, MA: Cell Press and Blackwell Press.
- Reddy, A. S. (2007). Alternative splicing of pre-messenger RNAs in plants in the genomic era. *Annual review of plant biology* **58**: 267-294.
- Rehfeldt, C., I. Fiedler, et al. (2000). Myogenesis and postnatal skeletal muscle cell growth as influenced by selection. *Livestock Production Science* **66**(2): 177-188.
- Rehfeldt, C., I. Fiedler, et al. (1993). It is possible to increase skeletal muscle fibre number in utero. *Bioscience reports* **13**(4): 213-220.
- Rudnicki, M. A., P. N. Schnegelsberg, et al. (1993). MyoD or Myf-5 is required for the formation of skeletal muscle. *Cell* **75**(7): 1351-1359.
- Ryu, Y. C., Y. M. Choi, et al. (2008). Comparing the histochemical characteristics and meat quality traits of different pig breeds. *Meat Science* **80**(2): 363-369.
- Sun, L., J. S. Trausch-Azar, et al. (2007). E2A protein degradation by the ubiquitin-proteasome system is stage-dependent during muscle differentiation. *Oncogene* **26**(3): 441-448.
- Sun, X. H., N. G. Copeland, et al. (1991). Id proteins Id1 and Id2 selectively inhibit DNA binding by one class of helix-loop-helix proteins. *Molecular and cellular biology* **11**(11): 5603-5611.
- Tanner, C. J., H. A. Barakat, et al. (2002). Muscle fiber type is associated with obesity and weight loss. *American journal of physiology. Endocrinology and metabolism* **282**(6): E1191-1196.
- Velloso, C. P. (2008). Regulation of muscle mass by growth hormone and IGF-I. *British journal of pharmacology* **154**(3): 557-568.
- Walters, E. H., N. C. Stickland, et al. (2000). MRF-4 exhibits fiber type- and muscle-specific pattern of expression in postnatal rat muscle. *American journal of physiology. Regulatory, integrative and comparative physiology* **278**(5): R1381-1384.
- Weintraub, H., S. J. Tapscott, et al. (1989). Activation of muscle-specific genes in pigment, nerve, fat, liver, and fibroblast cell lines by forced expression of MyoD. *Proceedings of the National Academy of Sciences of the United States of America* **86**(14): 5434-5438.
- Wigmore, P. M. and G. F. Dunglison (1998). The generation of fiber diversity during myogenesis. *The International journal of developmental biology* **42**(2): 117-125.
- Wilson, S. J., J. C. McEwan, et al. (1992). Early stages of myogenesis in a large mammal: formation of successive generations of myotubes in sheep tibialis cranialis muscle. *Journal of muscle research and cell motility* **13**(5): 534-550.

- Yaffe, D. and O. Saxel (1977). Serial passaging and differentiation of myogenic cells isolated from dystrophic mouse muscle. *Nature* **270**(5639): 725-727.
- Yoshiko, Y., K. Hirao, et al. (1996). Autonomous control of expression of genes for insulin-like growth factors during the proliferation and differentiation of C2C12 mouse myoblasts in serum-free culture. *Life sciences* **59**(23): 1961-1968.
- Zhang, M., P. D. Zamore, et al. (1992). Cloning and intracellular localization of the U2 small nuclear ribonucleoprotein auxiliary factor small subunit. *Proceedings of the National Academy of Sciences of the United States of America* **89**(18): 8769-8773.